DESIGN AND SIMULATION OF A HIGH-POWER DOUBLE-OUTPUT ISOLATED CUK CONVERTER

Among the transformer-less DC-DC converters, the superiority of the conventional Cuk converter is obvious in its good properties. However, the output power is limited for all transformer-less converter types including the conventional Cuk converter. In order to get more supplied power from this converter, some changes in its design were necessary. One of these modifications is to add a transformer to transfer more power and to separate the output side from the input side. Supply of some applications such as the DC link of modular multilevel inverters, e. g. cascaded H-bridge (CHB) topologies required more than one output. Hence, this paper is concerned with the design, analysis and simulation of an isolated dual-output modified Cuk converter. The proposed converter is designed to deliver a total output power of 2,000 W using only one modulating switch. A complete design and detailed analysis of the high-frequency transformer with the ANSYS Maxwell platform is presented in this paper. The modeling and simulation results of the high-frequency transformer are validated by the experimental implementation results and good agreement was obtained with a small percentage of errors less than 4 %. A set of analytical equations has been derived and presented in this paper to represent a mathematical model of the converter. In addition, the entire converter circuit was simulated and analyzed with MATLAB/Simulink. The simulation results were checked and compared to the findings of the mathematical model, yielding an excellent match with a percentage error of less than 2.15 %. Finally, when the presented converter was tested under various loads, including unbalanced load situations, a reasonable output voltage regulation was achieved, with the two output voltages being nearly identical with a deviation of less than 0.25 % under a severe unbalanced load condition of 150 %

Keywords: isolated Cuk converter, DC-DC converter, double-output high-power converter, high-frequency transformer

Yasir M. Y. Ameen
Corresponding author
Doctor of Philosophy in Electrical Engineering,
Lecturer*
E-mail: yasir_752000@uomosul.edu.iq
Harith Al-Badrani
Doctor of Engineer in Electrical Engineering, Lecturer
Department of Electronic Engineering
College of Electronics Engineering
Ninevah University
Right Coast, Mosul, Iraq
Mohamed N. Abdul Kadir
Doctor of Philosophy in Electrical Engineering,
Lecturer*
*Department of Electrical Engineering
College of Engineering
University of Mosul
Al Majmoaa str., Mosul, Iraq, 41002

1. Introduction

The conventional Cuk converter is well known in the realm of DC-DC converter applications. This converter possesses most of the features of the basic DC-DC converters. It is efficient, small in size and weight, inexpensive, reliable, has a simple control circuit, etc. The basic converters, i.e., buck, boost, and buck-boost, as well as the conventional Cuk converter, rely on storing energy in an inductor or capacitor. Therefore, the main disadvantages of all transformer-less DC-DC converters including the conventional Cuk are the limitation of their application to low to medium power and the lack of isolation between the input and output sides. To overcome these drawbacks, some design modifications are necessary. One of these modifications is to use a transformer by inserting it into the converter structure to maximize its output power and to separate the output side from the input side. In addition, feeding of some applications required DC-DC converters with more than one output besides the high power ability. For example, the modular multi-level CHB inverter is used in a wide variety of applications. It has been used successfully in high-power applications over the years [1, 2]. It necessitates multiple isolated in-put power supplies, which vary depending on the number of its levels. In some cases, controlled DC power supplies from DC-DC converters are used to power its input, but this increases the overall cost of the system and also decreases its reliability. It is therefore a major challenge for the switch-mode DC power supply designer to develop a converter with the ability to provide a high level of power with more than one output and each separately from one another and also from the input size based on only one power semiconductor switching device.

2. Literature review and problem statement

Many DC-DC converter topologies consisting of a single input and multiple outputs, which are based on buck, boost, buck-boost, Cuk, etc. are discussed in the literature. Most of these topologies have limited output power and no isolation property. A non-isolated DC-DC converter with a single input and double output (SIDO) was developed on the basis of the Cuk and SEPIC converter and highlighted in [3]. In [4], a novel DC-DC converter with a single input and multiple-output is proposed based on a boost converter,

but also with limited power capabilities and lack of isolation. A DC-DC converter limited to 180 W with two outputs is presented in [5] by coupling a SEPIC and a high-voltage multilevel boost converter, but the outputs are not isolated in this converter as well. The same system, but based on a buck-boost converter is explained in [6], while a buck non-isolated converter with double outputs and one input is presented in [7]. A non-isolated single-input and three-output DC-DC converter is provided in [8]. The presented converter has four switches and is also based on a buck converter. The non-isolated solar-powered zeta-buck-boost and SEPIC-Cuk are discussed in [9] for low power application. A simulation-based study is performed in [10] to obtain a mathematical model and a stationary model of a low-power Cuk converter-based LED drive using MATLAB software. The model was used to study the transient and steady state voltage and current properties. In addition, a control of the Cuk converter was developed in order to provide a constant voltage at the output regardless of the variation in the output parameters. For applications with low power consumption, a new protocol topology called isolated Cuk converter is introduced, which is fed to a BLDC (brushless direct current) motor drive [11]. The intermediate DC link voltage of the voltage source inverter, VSI, was controlled to regulate the speed of the BLDC machine. A modified Cuk converter for driving a switched reluctance motor (SRM) is proposed in [12]. In a similar vein, an isolated dual-output Cuk converter as the front-end converter for SRM drive is introduced in [13]. In addition, the proposed converters are used as a power factor correction (PFC) to improve the quality of the AC source. The modified converter configuration consists of two Cuk converters and each of them works separately for two half cycles of the supply voltage. The proposed converter generates two identical voltages via two output capacitors in order to feed a split-capacitor converter of a 4-phase SRM drive.

In [14], a generalized circuit averaging technique is used to obtain the frequency response of the open-loop transfer function for Cuk and SEPIC converters. The behavior of the converters in continuous current mode (CCM) was simulated with the LTSPICE software package. The paper concluded that the derived averaged models of the converters contribute to faster and easier simulation. A general overview of multiple-input DC-DC topologies is presented in [15], and another survey for single-input DC-DC topologies used with a microgrid DC system is done in [16]. Similarly, an overview of DC-DC converters using single-input multiple-output technology for low-power applications that are limited for LED lighting control is presented in [17].

The isolated single-input single-output Cuk converter is discussed in [18], and is considered an ideal solution for applications where isolated DC links are required. A Cuk converter with multiple isolated outputs and limited power capabilities is proposed in [19]. A non-isolated single-input multiple-output converter based on a hybrid converter configuration, which is designed by combining Cuk, boost and SEPIC, for renewable energy applications is proposed in [20]. This design uses only one switch but it does not provide isolation.

Table 1 summarizes the key features of the listed cited sources as well as their major drawbacks from the viewpoint of this work. It is clear that most of the earlier works in the literature either have multiple outputs but limited power rating or no isolation. In addition, some of these works have many modulating switches that complicate the gate drive circuit and incur additional losses, as well as the complexity of the transformer design in some of them.

Accordingly, the focus of this study is to show the design and simulation of a high-power 2,000 W SIDO isolated modified Cuk converter based on only one switching device. In the proposed converter, each output, as well as the input side, are completely isolated. It is, therefore, suitable to feed the intermediate circuits of a modular CHB inverter.

Table 1

A list of the most important points in the stated literature

Ref.	Converter Type	Switches number	Power Rating	Galvanic Isolation	SIMO	Main drawbacks compared to the present work
[3]	Cuk, SEPIC	2	Low	No	Yes	Low power, no isolation, more than one switch
[4]	Modified DC-DC	2	Low	No	Yes	
[5]	SEPIC/ Boost	1	Low	No	Yes	Low power, no isolation
[9]	Modified DC-DC	1	Low	No	Yes	
[6]	Buck-boost	3 for double output	Low	No	Yes	Low power, no isolation, large switches number
[7]	Buck	4	Low	No	Yes	Low power, no isolation, large switches number, i/p current discontinuity
[8]	Modified Buck	4	Low	No	Yes	
[10]	Cuk	1	Low	No	No	Low power, no isolation, SISO
[14]	Cuk	1	Low	No	No	
[11]	Bridgeless isolated Cuk	2	Medium	Yes	Yes	two switches, complexity of HF transformer design
[12]	Modified Cuk	1	Low	No	Yes	Low power, no isolation, two outputs with a common point
[13]	Modified Cuk	1	Medium	Yes	Yes	two outputs with a common point, high power not investigated
[18]	Isolated Cuk	3 for forward	High	Yes	No, SISO	large switches number, SISO
[19]	Cuk, Flyback Forward, SEPIC	1	Low	Yes	Yes	Low power, complexity of HF transformer design
[20]	Cuk, SEPIC	1	Low	No	Yes	Low power, no isolation
Present work	Modified Isolated Cuk	1	High	Fully isolated each o/p and i/p	Yes	–

3. The aim and objectives of the study

The aim of this study is to develop and evaluate a new SIDO fully isolated DC-DC converter based on a PWM-controlled single power transistor. The converter is designed to generate a nominal power of 1000 W for each output port, so the nominal power of the proposed converter is around 2000 W. The proposed converter is based on the conventional Cuk converter topology.

To achieve the aim, the following objectives were set:
– to develop a magnetic analysis, utilizing ANSYS Maxwell software, to design the converter's high-frequency transformers at operating frequency equal to 30 kHz;
– to conduct the mathematical analysis of the proposed converter circuit in order to derive the formulas of the voltages and currents of the converter elements;
– to perform a simulation study with the MATLAB Simulink platform to evaluate the performance of the proposed converter.

4. Materials and methods of research

4. 1. Methods
The following methods are used during the study:
– average model technique based on the switching state to derive a mathematical model of the proposed converter for the steady state;
– finite element method (FAM) for the analysis and simulation of the high-frequency transformer for the converter construction;
– discrete simulation method in MATLAB/Simulink Software for performing a discretization of the whole converter for a solution in fixed time steps.

4. 2. The proposed SIDO topology
The conventional Cuk converter is well known in the literature and is shown in Fig. 1. This converter possesses most of the advantages of other DC-DC converters, such as continuity of both input and output currents with very low ripple, simplicity of its gate drive circuit, and protection of the output side in case of switching failure due to the insulation feature of its capacitor.

Besides, the converter has the ability to step-up like boost converter or step-down the input voltage like buck converter. In any case and based on this converter, the SIDO isolated modified Cuk converter is proposed, as shown in Fig. 2. In principle, this topology allows converting the energy in both directions if antiparallel transistors are added with the secondary diodes D_{21}

and D_{22}. However, in this work, only the forward operation mode was considered with different loads and, consequently, different currents at the output. The backward operation mode with multiple inputs and a single output needs to be carefully examined and works only under certain restrictions of symmetry. This objective is beyond the scope of this paper. The two secondary windings in the forward operation mode can be used individually or can be connected in various configurations producing a higher voltage or current supply. To connect the secondary windings of the transformers, their rated values also have to be considered. In the double-output converter, C_1 is the energy transfer capacitor on the primary side, whereas, C_{21} and C_{22} are the energy transfer capacitors on the secondary side for two insulated outputs. L_1 represents the input inductance, and L_{21} and L_{22} represent the output inductances. During the Q_1 turn-off, the high di/dt, together with the leakage inductances on the primary side cause voltage spikes that can damage and even destroy the transistor. This adverse effect can be reduced to a great extent by implementing the careful design of the transformers and having a parallel connection of the transformers on the primary side, which will reduce the leakage inductance.
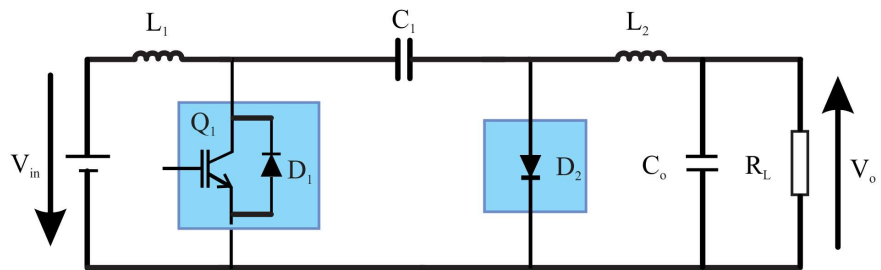

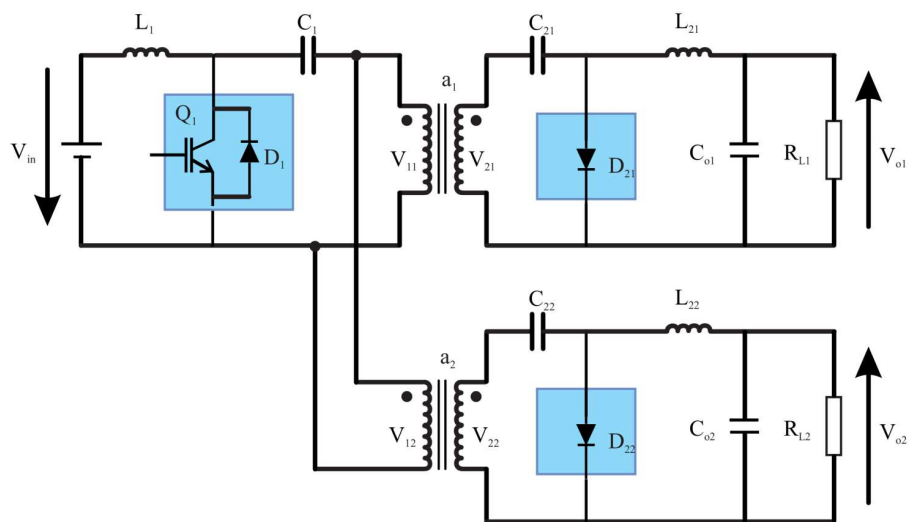Fig. 1. Conventional Cuk converter

Fig. 2. The proposed SIDO converter circuit topology

The steady-state analysis of the proposed converter is performed in the same way as the conventional Cuk converter [21]. For this, an average model technique based on the state of the switches is applied. Fig. 3, a, and Fig. 3, b show the circuit topology during ON and OFF state of $Q1$.
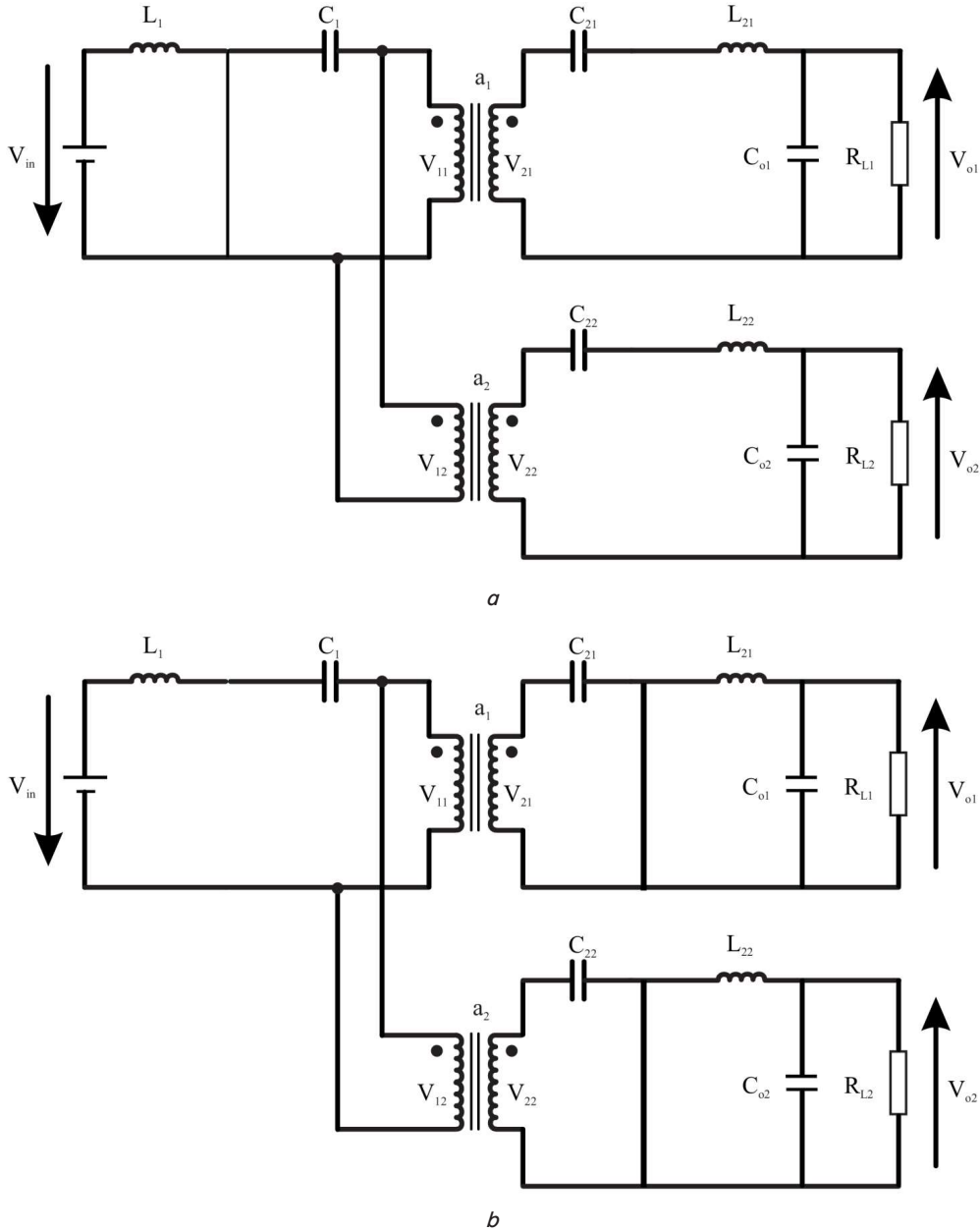
Fig. 3. Circuit topology: *a* — ON-state topology; *b* — OFF-state topology

Assuming the capacitor voltages V_{C1}, V_{C21}, and V_{C22} to be constant, this assumption is reasonably valid in practical circuits, and by equating the integral of voltages across the input and output inductors over one time period to zero, leads to the equilibrium voltage equation across $L1$ over one time period, so in the steady state, the average inductor voltages V_{L1}, V_{L21}, and V_{L22} are zero and given as:

$$V_{Lx(\text{ON})} \cdot t_{\text{ON}} + V_{Lx(\text{OFF})} \cdot t_{\text{OFF}} = 0, \tag{1}$$

where the subscript Lx indicates any inductor $L1$, $L21$, or $L22$; t_{ON} and t_{OFF} are the ON and OFF periods of switch $Q1$. Thus, for input inductor $L1$ coupled with $L21$, we obtain:

$$V_{in}\delta Ts + \left(V_{in} - V_{C1} - \frac{V_{C21}}{a_1 . \eta_1}\right)(1-\delta)Ts = 0, \tag{2}$$

and for $L1$ coupled with $L22$:

$$V_{in}\delta Ts + \left(V_{in} - V_{C1} - \frac{V_{C22}}{a_2 . \eta_2}\right)(1-\delta)Ts = 0, \tag{3}$$

(2) leads to:

$$a_1 \cdot \eta_1 \cdot V_{C1} + V_{C21} = \frac{a_1 \cdot \eta_1 \cdot V_{in}}{1-\delta}, \tag{4}$$

and (3) leads to:

$$a_2 \cdot \eta_2 \cdot V_{C1} + V_{C22} = \frac{a_2 \cdot \eta_2 \cdot V_{in}}{1-\delta}, \tag{5}$$

where a_1 and a_2 are the transformer 1 and transformer 2 turns ratio; respectively, η_1 and η_2 are the efficiency of transformer 1 and transformer 2; respectively.

For the output inductor $L21$, the equilibrium voltage equation is:

$$(-a_1 \cdot \eta_1 V_{C1} + V_{C21} - V_O)\delta Ts + (-V_O)(1-\delta)Ts = 0, \tag{6}$$

(6) leads to:

$$a_1 \cdot \eta_1 \cdot V_{C1} + V_{C21} = \frac{V_o}{\delta}, \tag{7}$$

Again, for L22, we obtain:

$$(-a_2 \cdot \eta_2 \cdot V_{C1} + V_{C22} - V_O)\delta Ts + (-V_O)(1-\delta)Ts = 0, \tag{8}$$

$$a_2 \cdot \eta_2 \cdot V_{C1} + V_{C22} = \frac{V_o}{\delta}. \tag{9}$$

Thus, the voltage gains or output voltage to input voltage transfer function of the two converter outputs are determined by equating (4) with (7) and (5) with (9):

$$V_{o1} = a_1 \frac{\eta_1 \delta}{1-\delta} V_{in}. \tag{10}$$

$$V_{o2} = a_2 \frac{\eta_2 \delta}{1-\delta} V_{in}. \tag{11}$$

The input current is derived using the hypothesis of a lossless circuit as follows:

$$I_i = a_1 \frac{\eta_1 \delta}{1-\delta} I_{o1} + a_2 \frac{\eta_2 \delta}{1-\delta} I_{o2}. \tag{12}$$

The output average power for the two outputs can be obtained as:

$$P_{o1} = \frac{V_{o1}^2}{R_{L1}}, \tag{13}$$

$$P_{o2} = \frac{V_{o2}^2}{R_{L2}}. \tag{14}$$

The ripple of currents inductors, Δi_{L1}, Δi_{L21} and Δi_{L22}, during the ON interval or the OFF interval can be determined as follows:

$$\Delta i_{L1} = \frac{V_{in}}{L_1} \cdot \delta \cdot T_S, \tag{15}$$

$$\Delta i_{L21} = \frac{V_O}{L_{21}} \cdot (1-\delta) \cdot T_S. \tag{16}$$

$$\Delta i_{L22} = \frac{V_O}{L_{22}} \cdot (1-\delta) \cdot T_S. \tag{17}$$

4. 3. Modeling and design of the main transformer

To obtain the parameters of the main converter transformers, a 3D model was developed based on the ANSYS MAXWELL software. Fig. 4 shows the transformer dimensions, which are taken from the datasheet in [22], where the transformer core is made of N72-type ferrite and Litz wire is used. The primary and secondary windings are rolled up together and overlapped to reduce leakage flux and thus transformer losses.

Table 2 shows the details of the design parameters considered.

The meaning and description of the symbols used can also be seen in Fig. 4. In this case, the turns ratio of the two transformers is assumed to be equal and equal to 1.
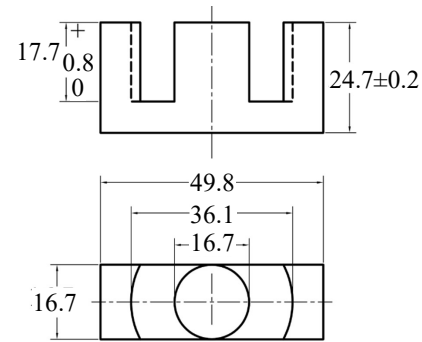
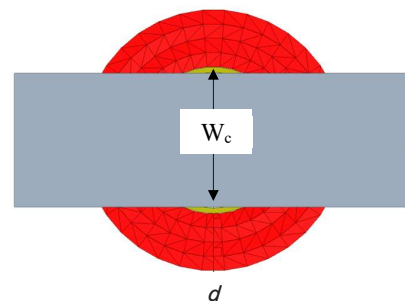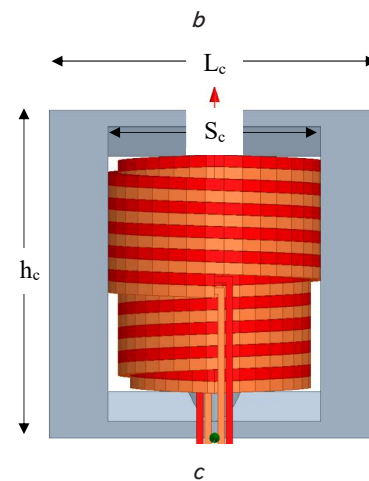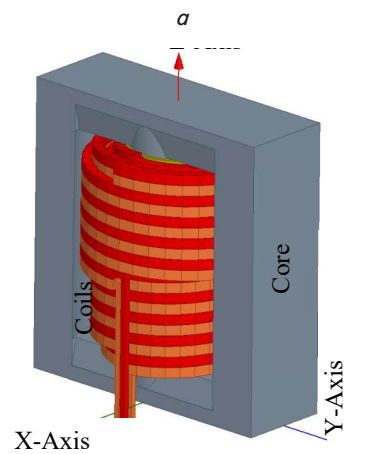Fig. 4. The geometry of the main transformer: a — Core dimension; b — 3D view; c — Front view; d — Top view

Table 2

Main transformer specifications

Parameter	Symbol	Value
Core length	L_c	49.8 mm
Core width	W_c	16.7 mm
Core height	h_c	49.4 mm
Core space	S_c	32 mm
Number of primary turns	Np	32
Number of primary turns	Ns	32

5. The proposed SIDO converter results

5. 1. Transformer magnetic design results

First, the transformer output was analyzed using the "Magnetostatic" solution type in ANSYS MAXWELL software to obtain the parameters of primary self-inductance, secondary self-inductance, and mutual inductance between two windings (L_1, L_2, M), in case of injecting a current of 5.1A RMS to the transformer primary winding. Table 3 displays the results obtained.

Fig. 5, *a* shows the flux distribution inside and outside the transformer core. The effectiveness of the designed transformer can also be assessed by noting the magnetic field in the directions of the *x*, *y*, and *z* axes, as shown in Fig. 5, *b*–*e*.

In fact, the design of the high-frequency transformer of the converter is considered a critical. Therefore, in order to validate the developed model of the high-frequency transformer presented in Section 4. 2 and to confirm the results obtained in Table 3, the transformer design was implemented in the laboratory according to the data in Table 2, as shown in Fig. 6. The results were obtained by measuring the inductance at a high-frequency setting obtained with LCR meter model GW Instek LCR-816. The transformer inductances were $L1=4.3226$ mH and $L2=4.3168$ mH. These values come very close to the simulation results of $L1$ and $L2$: $L1=4.493925$ mH and $L2=4.494732$ mH. To describe this closeness in numerical language, the percentages of error for $L1$ and $L2$ were calculated to be 3.81 % and 3.96 %, respectively.
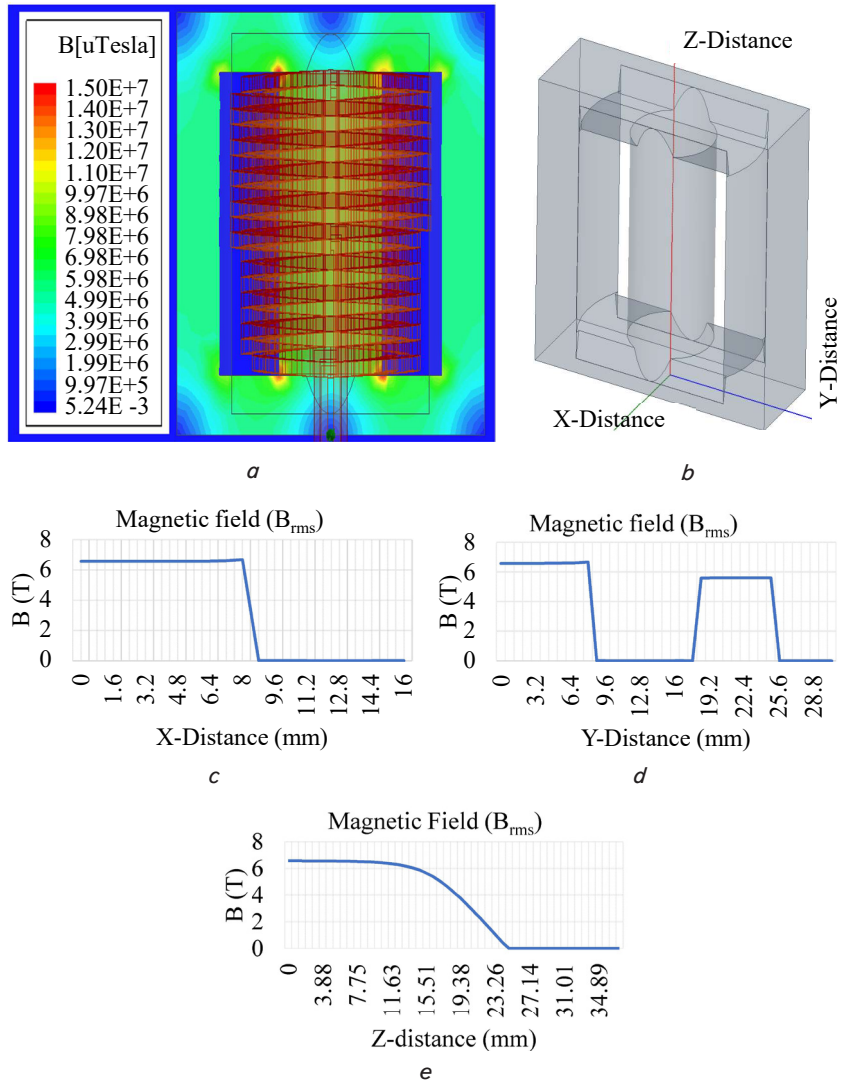
Fig. 5. Magnetic flux distribution inside and outside the transformer core: $a - B_{rms}$ for core; $b -$ View direction of B_{rms}; $c - B_{rms}$ of X-axis; $d - B_{rms}$ of Y-axis; $e - B_{rms}$ of Z-axis
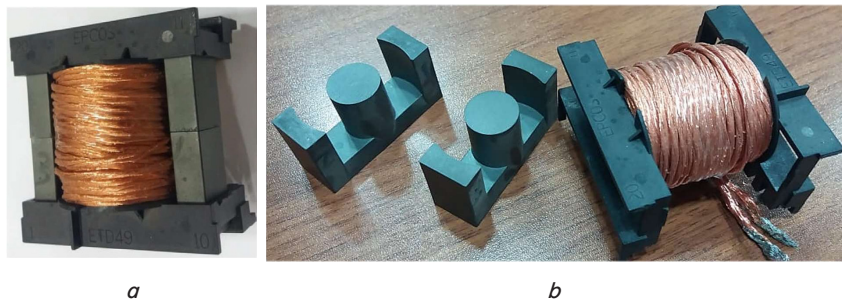
Fig. 6. Implementation of the high-frequency transformer: $a -$ assembled with the core; $b -$ disassembled without a core

5. 2. Mathematical analysis results

To validate the derived equations shown in Section 4. 1, two different operating modes were taken into account when evaluating the converter namely a step-up and a step-down in the forward operation mode. Fig. 7, *a* depicts the total power output of the converter, the sum of the power of the two outputs, as a function of the duty cycle. However, in the step-up operation mode $d \geq 0.5$, the output voltage was kept at

Table 3

Calculated parameters of the transformer

L_1, mH	L_2, mH	M, mH	CuplCoef. (k)	Leakage inductance, µH
4.493925	4.494732	4.493055	0.999717	0.87

its desired value of 200 V, $V_{in}=V_{in}(d, V_{out})$, and the load resistances were symmetrically adapted until the maximum input current of 10 A was reached. In the range of $d \leq 0.5$ (operation as a step-down converter), the input voltage was constant at 200 V, $V_{out}=V_{out0}(d, V_{in})$, and the load was adapted until the maximum output current of 5 A in each output was obtained. In Fig. 7, the input and output voltages and currents are also plotted as a function of duty cycle.

However, the results of the voltages, currents and output powers were also confirmed using simulation results, as can be seen in the next section.
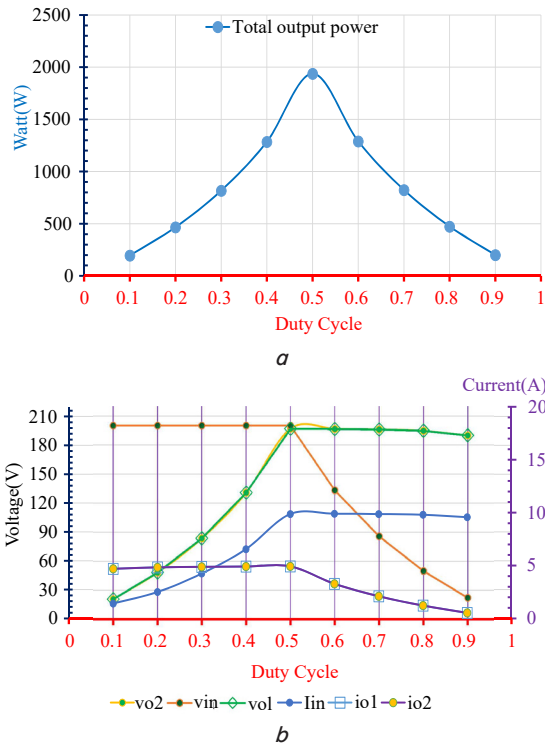

a

b

Fig. 7. Step-up and step-down operation modes of SIDO isolated Cuk converter for different duty cycles: *a* — total output power; *b* — corresponding voltages and currents

5. 3. Converter simulation results

A simulation study was carried out to understand the behavior of the entire converter circuit. MATLAB/Simulink software was used for simulation and analysis purposes. The ready-made models of the circuit elements in the MATLAB library were used.

The currents of the circuit elements including the input inductor current i_{L1}, the output inductors current i_{L21} and i_{L22}, the input capacitor current i_{C1}, the current of the output capacitors i_{C21} and i_{C22}, the diode currents i_{D1} and i_{D2}, and the two output currents i_{o1} and i_{o2} are shown in Fig. 8, whereas, the voltages of these elements for the same time interval are shown in Fig. 9. The figure includes the gate signal voltage (Gate), the switching voltage v_Q, the diode voltages v_{D1} and v_{D2}, the primary voltage v_{p1}, the secondary voltages v_{s1} and v_{s2}, and also the input supply voltage v_i and the output voltages v_{o1} and v_{o2}.

When the converter circuit was regulated with PWM (pulse width modulation) and a signal duty cycle of 0.5, the previous waveforms were captured. To operate the converter in step-up mode, δ must be more than 0.5, while δ must be less than 0.5 to operate the converter in step-down mode. To prove these results as well as make a validation of the math-

ematical representation given in section (4.1), it is necessary to compare some of the aforementioned results with the outcomes of the mathematical equations. Therefore, assuming $R_{L1}=R_{L2}=40\Omega$, $a_1=a_2=1$, $\eta_1=\eta_2=98.5\%$ and $\delta=0.5$, the following results are obtained for V_{o1}, V_{o2}, I_{in}, P_{o1}, P_{o2}, Δi_{L1}, Δi_{L21} and Δi_{L22} using equations (10) to (17). The last equations outcomes are compared with the simulation results of Fig. 8 and Fig. 9 as shown in Table 4.

The converter circuit was also tested with different loads and currents in the output. The results for each of the two outputs in terms of voltage, current, and power are documented in Table 5 with the loads $R_{L1}=40\Omega$, and $R_{L2}=60\Omega$.

It can be seen that the voltage at both outputs is well regulated even though the loads were unbalanced, where $RL2=150\%$ of $RL1$. The deviation between V_{o1} and V_{o2} is about 0.25 %.

Table 4

Simulation and mathematical model results validations

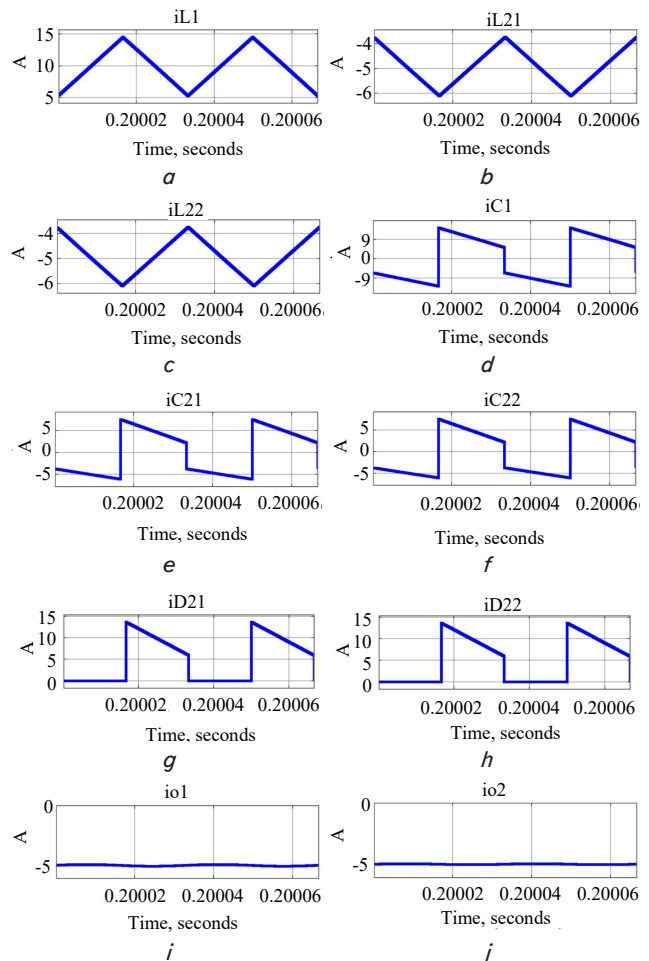| Result type \ Variable	V_{o1} (V)	V_{o2} (V)	I_{in} (A)	P_{o1} (W)	P_{o2} (W)	Δi_{L1} (A)	Δi_{L21} (A)	Δi_{L22} (A)
Mathematical	197	197	9.70	970.2	970.2	9.26	2.32	2.32
Simulation	196.9	196.9	9.87	969.1	969.1	9.06	2.32	2.32
Absolute Error %	0.051	0.051	1.75	0.11	0.11	2.15	0	0

Fig. 8. The currents of the circuit elements: *a* — inductor L1 current; *b* — inductor L21 current; *c* — inductor L22 current; *d* — capacitor C1 current; *e* — capacitor C21 current; *f* — capacitor C22 current; *g* — diode D1 current; *h* — diode D2 current; *i* — output1 current; *j* — output2 curren
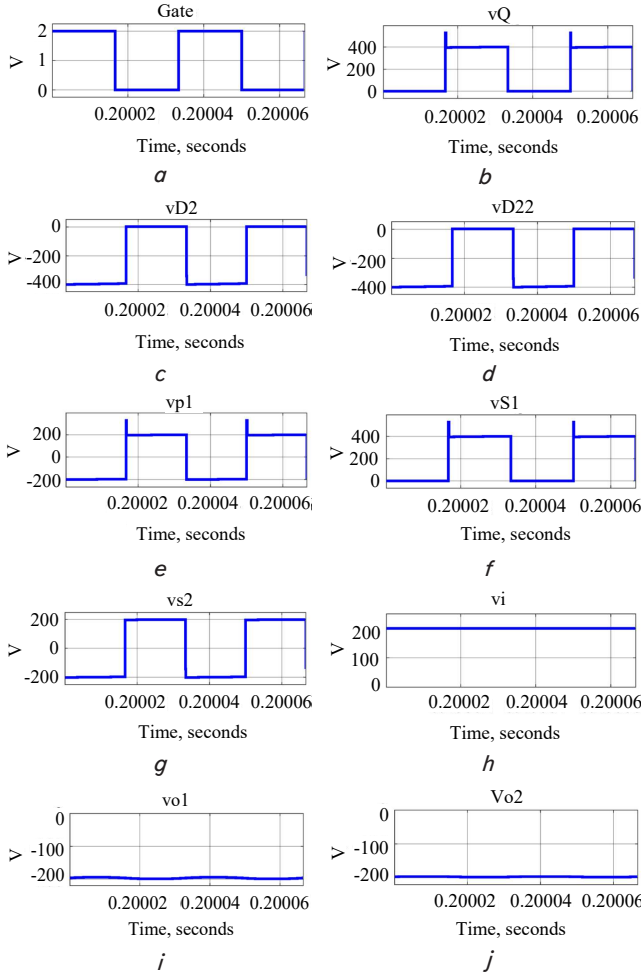
Fig. 9. The voltages across the circuit elements: *a* — gate signal; *b* — transistor voltage; *c* — D1 voltage; *d* — D2 voltage; *e* — transformer primary voltage; *f* — transformer1 secondary voltage; *g* — transformer1 secondary voltage; *h* — input supply voltage; *i* — output1 voltage; *j* — output2 voltage

Table 5

Input and output voltage, current, power, and load resistance for unbalanced conditions; RL1=40 Ω, RL2=60 Ω

Variable name	Voltage [V]	Current [A]	Power [W]
Input	200	8.26	1652.0
Output 1	196.9	4.924	969.53
Output 2	197.4	3.291	649.64

6. Discussion of the design and simulation results of the proposed SIDO converter

The design of the high-frequency transformer is the critical point in the overall converter design. Performing a magnetic analysis with the ANSYS Maxwell software was useful to create and obtain the parameters of the electrical model of the transformer. Some aspects like the coiling and wrapping of the primary and secondary windings are effective to reduce the leakage inductance and increase the coupling coefficient (k). It is clear from Table 3 that the leakage inductance has a small value at 0.87 µH and the coupling coefficient has a high value at 0.999717. The selection of transformer wire type is also an important issue. Litz wire was recommended for inductor and transformer construc-

tion when operating in the high-frequency range to reduce eddy current losses.

However, the converter is proposed to be used as an intermediate DC link between CHB multilevel inverter and renewable energy source. Fig. 5 depicts this scenario, assuming that the target voltage for CHB is 200 V. So, if the output of the renewable energy source is dropped, the proposed converter must operate in step-up mode>0.5. Therefore, as it is shown, the converter output is almost equal to 200 V. If the renewable energy source voltage, which is the input of the proposed converter is almost steady at 200 V, then the converter can be utilized as step-down to produce voltage less than 200 V, if it is desired, by making δ<0.5. In both cases, the total output power of the converter was equal to the sum of the power of both outputs.

The MATLAB simulation results show the detailed operational analysis by logging and capturing the instantaneous voltage and current waveforms of all converter elements. Fig. 6, *a* confirms the continuity mode of the converter presented like the conventional Cuk circuit. While Fig. 6, *b* and Fig. 6, *c* show that the current style of both output currents was also in continuous current mode. In the ideal case of the design of the converter elements, the load voltage at the power transistor is 2vin=400 V. However, when parasitic elements in circuit elements are considered, Fig. 7, *b* indicates that this stress equals the overshoot plus the usual stress, at 0.5, equals 527 V. The transformer leakage and circuit stray inductance are almost entirely responsible for the overshoot voltage during switching transitions over the converter's transistor. By properly wiring circuit elements and improving the design of a high-frequency transformer, this stress can be effectively decreased. As shown in Table 5, the probability of an unequal load or unbalanced load condition is also considered. R_{L1}=40 and R_{L2}=60 are two uneven loads evaluated; despite this unbalance condition, the output voltages were V_{o1}=196.9 V and V_{o2}=197.4 V, which were virtually identical.

Finally, it's worth noting that the proposed converter's function in this study was limited to the forward operation. Consequently, this research may be further explored by looking at converter circuit operation in backward. Furthermore, the proposed converter outputs can easily be expanded to more than two, whereby the total output power can be increased.

7. Conclusions

1. In this paper, the main converter transformer was modeled and designed using the ANSYS Maxwell software. The results of the experimental implementation confirm the simulation results obtained. The percentage of errors was less than 4 % for both primary and secondary inductance. Coiling and wrapping the primary and secondary windings of the transformer in parallel was effective in increasing the coupling coefficient so that k=0.999717 was found very close to unity. Thus, a small value of the leakage inductance is obtained and was equal to 0.87 mH. Consequently, a minimal leakage inductance means minimizing the voltage peaks on the modulating switching device.

2. A set of analytical equations has been derived and presented in this paper to represent a mathematical model of the converter. These equations can be used in designing the proposed converter circuit. The outcomes of the mathematical equations confirm the efficiency of using an averaging model analysis technique to represent DC-DC converter circuits.

3. The results of the MATLAB simulation showed that the design of the presented converter was effective in serving a high-power load up to 1,000 W for each output terminal. The examination of the input and output currents showed their operation in the CCM. The simulation results were validated and compared to the mathematical model results and a good match was obtained, with a percentage error of less than 2.15 percent. Finally, when the presented converter was tested under various loads, including unbalanced load situations, a reasonable output voltage regulation was attained where the two output voltages were almost the same with a deviation of less than 0.25 % under a severe unbalanced load condition that was R_{L2}=150 % of R_{L1}.

References

1. Sarrazin, B., Rouger, N., Ferrieux, J. P., Avenas, Y. (2011). Benefits of cascaded inverters for electrical vehicles' drive-trains. 2011 IEEE Energy Conversion Congress and Exposition. doi: https://doi.org/10.1109/ecce.2011.6063950

2. Maaroof, H. S., Al-Badrani, H., Younis, A. T. (2021). Design and simulation of cascaded H-bridge 5-level inverter for grid connection system based on multi-carrier PWM technique. IOP Conference Series: Materials Science and Engineering, 1152 (1), 012034. doi: https://doi.org/10.1088/1757-899x/1152/1/012034

3. Marjani, J., Imani, A., Hekmati, A., Afjei, E. (2016). A new dual output DC-DC converter based on SEPIC and Cuk converters. 2016 International Symposium on Power Electronics, Electrical Drives, Automation and Motion (SPEEDAM). doi: https://doi.org/10.1109/speedam.2016.7525949

4. Guler, N., Irmak, E. (2016). Design and application of a novel single input – Multi output DC/DC converter. 2016 IEEE International Conference on Renewable Energy Research and Applications (ICRERA). doi: https://doi.org/10.1109/icrera.2016.7884492

5. Ranjana, M. S. B., Reddy, N. S., Kumar, R. K. P. (2014). A novel sepic based dual output DC-DC converter for solar applications. 2014 POWER AND ENERGY SYSTEMS: TOWARDS SUSTAINABLE ENERGY. doi: https://doi.org/10.1109/pestse.2014.6805309

6. Boora, A. A., Zare, F., Ghosh, A. (2011). Multi-output buck–boost converter with enhanced dynamic response to load and input voltage changes. IET Power Electronics, 4 (2), 194. doi: https://doi.org/10.1049/iet-pel.2009.0269

7. Aden, İ. A., Kahveci, H., Şahin, M. E. (2017). Single Input, Multiple Output DC-DC Buck Converter for Electric Vehicles. Turkish Journal of Electromechanics & Energy, 2 (2), 7–13.

8. Sabbarapu, B. K., Nezamuddin, O., McGinnis, A., dos Santos, E. (2016). Single-input multiple-output synchronous DC-DC buck converter. 2016 IEEE Energy Conversion Congress and Exposition (ECCE). doi: https://doi.org/10.1109/ecce.2016.7855438

9. Akhil Raj, P., Arya, S. R. (2020). Solar supplied two-output DC–DC converters in the application of low power. Automatika, 62 (2), 172–186. doi: https://doi.org/10.1080/00051144.2020.1805859

10. Surya, S., Patil, V. (2019). Cuk Converter as an Efficient Driver for LED. 2019 4th International Conference on Electrical, Electronics, Communication, Computer Technologies and Optimization Techniques (ICEECCOT). doi: https://doi.org/10.1109/iceeccot46775.2019.9114648

11. Bist, V., Singh, B. (2015). A Unity Power Factor Bridgeless Isolated Cuk Converter-Fed Brushless DC Motor Drive. IEEE Transactions on Industrial Electronics, 62 (7), 4118–4129. doi: https://doi.org/10.1109/tie.2014.2384001

12. Anand, A., Singh, B. (2019). Modified Dual Output Cuk Converter-Fed Switched Reluctance Motor Drive With Power Factor Correction. IEEE Transactions on Power Electronics, 34 (1), 624–635. doi: https://doi.org/10.1109/tpel.2018.2827048

13. Anand, A., Singh, B., Chandra, A., Al-Haddad, K. (2018). Isolated Cuk Converter with Two Symmetrical Output voltages For SRM Drive. 2018 IEEE Wireless Power Transfer Conference (WPTC). doi: https://doi.org/10.1109/wpt.2018.8639257

14. Surya, S., Williamson, S. (2021). Generalized Circuit Averaging Technique for Two-Switch PWM DC-DC Converters in CCM. Electronics, 10 (4), 392. doi: https://doi.org/10.3390/electronics10040392

15. Gavris, M., Cornea, O., Muntean, N. (2011). Multiple input DC-DC topologies in renewable energy systems - A general review. 2011 IEEE 3rd International Symposium on Exploitation of Renewable Energy Sources (EXPRES). doi: https://doi.org/10.1109/expres.2011.5741805

16. Dahale, S., Das, A., Pindoriya, N. M., Rajendran, S. (2017). An overview of DC-DC converter topologies and controls in DC microgrid. 2017 7th International Conference on Power Systems (ICPS). doi: https://doi.org/10.1109/icpes.2017.8387329

17. Chinchero, H. F., Alonso, J. M. (2020). Review on DC-DC SIMO Converters with Parallel Configuration for LED Lighting Control. 2020 IEEE ANDESCON. doi: https://doi.org/10.1109/andescon50619.2020.9272083

18. Li, C., Herrera, L., Jia, J., Fu, L., Isurin, A., Cook, A. et. al. (2014). Design and Implementation of a Bidirectional Isolated Ćuk Converter for Low-Voltage and High-Current Automotive DC Source Applications. IEEE Transactions on Vehicular Technology, 63 (6), 2567–2577. doi: https://doi.org/10.1109/tvt.2013.2294599

19. Singh, S., Bhuvaneswari, G., Singh, B. (2010). Multiple output SMPS with improved input power quality. 2010 5th International Conference on Industrial and Information Systems. doi: https://doi.org/10.1109/iciinfs.2010.5578673

20. Barath J.G., N., Soundarrajan, A., Stepenko, S., Bondarenko, O., Padmanaban, S., Prystupa, A. (2020). Hybrid Multiport Converter for High Step-Up Renewable Energy Applications. 2020 IEEE KhPI Week on Advanced Technology (KhPIWeek). doi: https://doi.org/10.1109/khpiweek51551.2020.9250178

21. Bryant, B., Kazimierczuk, M. K. (2003). Derivation of the Cuk PWM DC-DC converter circuit topology. Proceedings of the 2003 International Symposium on Circuits and Systems, 2003. ISCAS '03. doi: https://doi.org/10.1109/iscas.2003.1205013

22. Data Sheet. ETD49/25/16. ETD cores and accessories (2008). Ferroxcube. Available at: http://ferroxcube.home.pl/prod/assets/etd49.pdf

EXPERIMENTAL DEPENDENCES OF MEASUREMENT DATA ON THE VOLUME OF INHALED AIR IN MULTI-FREQUENCY ELECTRICAL IMPEDANCE TOMOGRAPHY

Grayr Aleksanyan
PhD
Department Information and Measurement Systems and Technologie
Platov South-Russian State Polytechnic University (NPI)
Prosveshcheniya str., 132, Novocherkassk, Russian Federation, 346428
E-mail: graer@yandex.ru

This paper proposes an approach to modeling the process of artificial ventilation of human lungs by their controlled filling with a fixed volume of air, using an incentive spirometer Coach 2. This makes it possible to simulate the ventilation process for a healthy person and to link the assigned respiratory volume to measurement data. The results of experimental studies of the developed system of multifrequency electric impedance tomography are presented. The tests were performed for the frequency range from 50 kHz to 400 kHz (with a pitch of 50 kHz) at assigned respiratory volumes from 500 ml to 4,000 ml (with a pitch of 500 ml) for five inhalation/exhalation cycles. The scheme of research: active inhalation – passive exhalation, the number of tested volunteers – 3 people from the developers of the system. As a result, the dependences of the measured values of changes in potentials on the frequency of injected current for different respiratory volumes in three test participants without pathologies of the respiratory function and the external respiration function were obtained. The obtained results of the experimental studies show that there is a dependence of the value of the measurement data both on the volume of inhaled air and on the frequency of the injected current. This feature can be used to develop a number of medical devices for personalized monitoring of human lung function. It was also revealed that there are frequencies at which the maximum spread of measurement data according to the results of a series of repeated experiments is observed. At the same time, the nature of the change in the measurement data of the EIT at an increase in the volume of inhaled air is the same for all test participants. It is assumed that this feature can also be used to increase the EIT personalization degree

Keywords: electric impedance tomography, multifrequency, measurement data, respiratory volumes, experimental studies, conductivity

1. Introduction

Electrical impedance tomography (EIT) makes it possible to visualize the distribution of ventilation (that is, air filling) of human lungs by assessing the changes in the reconstructed transthoracic impedance [1]. This method can be used both in assessing the parameters of independent breathing and at artificial ventilation of lungs (AVL) [2]. Based on the obtained measurement data and their processing, a user is given a dynamic image reflecting the change in air filling in the considered areas of the lungs. Since obtained images depend on a change in the air content in the analyzed section, they can be characterized as functional, rather than anatomical (unlike, for example, spiral computed tomography or magnetic resonance tomography). One of the major problems that complicate the clinical application of the EIT method is a low degree of consideration of its parameters of exposure (especially frequency and force of injected current) for a particular patient. The EIT devices existing in the market do not provide this functionality and, accordingly, are limited in their capabilities in terms of advanced monitoring of lung functioning. This is due to differences in the structure and composition of the body, as well as in the activity of the entire respiratory system of a person as a whole and his lungs, in particular.

Overcoming the problems of clinical application of the EIT systems is possible with the introduction into practice of multi-frequency EIT (MF EIT) systems, which allow taking into consideration the dependence of changes in impedance of tissues of a human body on the frequency of the injected current. Thus, it becomes possible to take into consideration additional objective information about the object of study. This makes it possible to differentiate the subjects into groups, as well as to identify the structure of the object and the processes that take place (for example, the function of human lungs, the activity of the cardiovascular system, etc.).

At the same time, there is a problem of preclinical approbation of medical and technical means of the MF EIT and their study on living objects, including humans. This creates a number of difficulties in terms of research into the applicability of the MF EIT for the tasks of assessing the functional state of the lungs of patients with respiratory support. In this regard, there is a need to perform research into the methods and algorithms of the MF EIT not abstractly or using models, but under real conditions. This is especially important for obtaining measurement information in situations where further operation of the MF EIT systems is planned. One of the key areas of clinical use of the EIT is the monitoring of lung function of patients connected to the AVL apparatus.

That is why it is expedient to study and evaluate the work of the developed algorithms and the created MF EIT devices for conditions of intensive care units. At the same time, there is a major contradiction: on the one hand, to obtain initial data, it is necessary to perform the MF EIT simultaneously with the AVL, and on the other hand, it is impossible to connect the ventilator to a healthy person. The relevance of the solutions proposed in the paper lies in the practical implementation of the method for obtaining measurement data using the MF EIT method. The proposed method of controlled filling of lungs with a fixed volume of air while performing multi-frequency electric impedance tomography makes it possible to simulate the process of ventilation on a healthy person. In this case, the active element that controls the processes of inhalation and exhalation is a test participant who uses an incentive spirometer for research purposes. Thus, it becomes possible to conduct the MF EIT on a healthy person without connecting him to the AVL apparatus. This enables expanding the possibilities of studying the method. Thanks to this, it is possible to conduct preclinical studies of new methods, algorithms, and devices of the MF EIT under various AVL modes on healthy people. In addition, this approach allows identification of the problems of the practical use of the MF EIT systems for planning and conducting clinical examinations of the patients in intensive care units.

2. Literature review and problem statement

In clinical practice, it is important to be able to conduct non-invasive long-term bedside monitoring of air filling of the lungs of a patient connected to the AVL. Changes in such parameters as respiratory volumes and the magnitude of positive exhalation end pressure (PEEP) in patients with mechanical ventilation of lungs have a significant impact on their functional state [3, 4]. At the same time, an incomparably smaller number of scientific works are devoted to the study of the process of air filling of the lungs at independent breathing of a person with the use of the MF EIT method. Moreover, the problems associated with the simultaneous change in both the parameters of breathing and the parameters of the impact (force and frequency of electric current) almost are not studied. For example, paper [3] studies the relationship between changes in respiratory volume and electrical impedance (obtained using the EIT method) and the changes in positive pressure at the end of exhalation of the studied object who is connected to the AVL. However, the issues related to how various indicators of respiratory volumes affect the recorded EIT data, both at independent and spontaneous breathing, remained unresolved in this paper. This is especially important, as it makes it possible to assess the sensitivity of the EIT method to the problems under consideration. An option for overcoming the relevant difficulties is the study performed in [4]. In it, the authors evaluated the boundary possibilities of the EIT method for visualizing the ventilation process at the AVL with small respiratory volumes. At the same time, within the framework of the research and the obtained results, the authors did not take into consideration the electrical properties of the tissues of the studied objects themselves. This issue is important, as it imposes a number of restrictions in terms of selecting an adequate mode of the EIT injection for a particular field of study and does not take into consideration its composition and structure. It is noted that, despite the known

limitations of the method, the EIT has great advantages in monitoring the lungs of a patient with respiratory complications who has mechanical ventilation. At the same time, as well as in [3], the issues of studying the respiratory volumes of patients without lung pathologies during independent breathing, when it is possible to vary the parameters of the effect of EIT in a wider range, remained unresolved. For example, the implementation of the multi-frequency function in EIT systems makes it possible to personalize all EIT activities, taking into consideration objective and reliable information about the object of study.

Papers [5, 6] showed that monitoring based on the EIT can be a source of valuable data on ventilation and perfusion function of lungs. Thus, paper [5] explores the possibilities of monitoring EIT of both the patients on mechanical ventilation of lungs and the patients who retain the function of independent breathing. It should be noted that the paper conducts the research into the parameters of independent breathing of patients with various pathologies of lungs and respiratory tract (asthma, chronic obstructive pulmonary disease, cystic fibrosis). At the same time, the authors did not consider the possibility of applying EIT monitoring of the lungs to the patients who do not have pathologies of the respiratory system. The paper does not disclose the parameters of EIT research, as well as their impact on the data obtained. Article [6] presents the results of studies on the use of the EIT for monitoring the respiratory volumes of animals (anesthetized horses during surgery). The results of clinical studies that confirm the possibility of recording respiratory volumes with the help of EIT are shown. However, like paper [5], it does not study how the obtained data depend on the parameters of exposure during the EIT. The studies similar to [5, 6] explore the problems of joint clinical use of the AVL and EIT systems. However, most of them do not solve the problems of increasing the personalization of the EIT method, including those based on the implementation of the MF EIT function. At the same time, the MF EIT is one of the promising areas for increased reliability. All this suggests that new studies are needed to establish general patterns and features of the MN EIT to solve the problems of monitoring the functional state of the lungs.

Paper [7] solves the issues of using a portable EIT device for monitoring the respiratory function of a person during apnea and subsequent hypoventilation. The importance and necessity of quantitative methods of assessment in the diagnosis of diseases are shown. The authors have developed a device that determines the respiratory volumes, the position of the body of the examined patient, the sounds made by a patient. The device also records the electrical activity of the heart (ECG) and pulse oximetry (SPO2). Analyzing the obtained results, it can be concluded that the measurement data of the EIT can complement the existing tools for monitoring lung activity. Accordingly, there is a practical need for methods and algorithms of EIT personalization. This will make it possible to overcome one of the main shortcomings of the device proposed by the authors – to assess the ventilation function of the lungs. Thus, the capabilities of the device and the scope of its application will be significantly expanded.

Research [8] explores one of the directions of the MF EIT, its diagnostic value both at mechanical ventilation and at independent breathing. The disadvantages of the paper include a narrow range of frequencies of injected current and the declared possibility of applying current up to 10 mA. In

addition, the possibility and degree of influence of the EIT parameters on the results of the study are not disclosed and are described in general phrases. Research [9] is devoted to the study of the process of independent breathing using the EIT after extubating a patient. The paper shows the diagnostic and prognostic value of the obtained measurement data. This article, due to the natural causes, does not reflect the effect of variation of respiratory volumes on recorded data, nor discloses the parameters of the EIT examination.

Thus, the conducted analysis of the current state of the problem revealed a number of unresolved issues related to the assessment of the dependence of respiratory volumes and parameters of the EIT examination. It does not pay sufficient attention to conducting EIT examination of the healthy objects without pathologies with the ability to change the parameters of air filling of lungs within a wide range with a simultaneous change in the frequency of the injected current. This is important for determining additional technical limitations of the EIT method, as well as for improving the efficiency of using the MF EIT systems. The current situation may be the result of the understandable focus of teams of researchers and developers primarily on the problems of patients with pathologies. However, as noted earlier, this approach does not make it possible to obtain additional data on the range of sensitivity of the EIT method to changes in respiratory volumes and the frequency of injected current for a given object of research.

All this makes it possible to assert that continuous monitoring lungs using the method of the MF EIT allows personalizing the tactics of treatment of respiratory complications in the postoperative period to a greater extent. However, the issues of practical implementation of the MF EIT remain unresolved, taking into consideration the specifics of the field of application. The greatest attention should be paid to the postoperative period, in which the main changes in lung function are observed. In this regard, there are problems of theoretical and algorithmic support for the personalization of the EIT research. It is advisable to conduct studies devoted to the exploration of the features of recorded EIT data at different frequencies of injected current and at different values of respiratory volume.

3. The aim and objectives of the study

The purpose of the study is an experimental assessment of the dependence of recorded measurement data on the volumes of inhaled air at the MF EIT. This will make it possible to assess the applicability of the proposed IMS of MF EIT in the problems of personalized MF EIT of lungs at the preclinical stage of trials. The practical implementation of the obtained research results will enhance the effectiveness of the clinical application of the technology of pre-and postoperative monitoring of lung function using the MF EIT method.

To achieve the set goal, it is necessary to solve the following problems:

– to propose a general plan of experimental research;

– to conduct experimental studies to determine the dependence of measurement data on the volume of inhaled air and the frequency of injected current;

– to perform processing and analysis of the obtained measurement information;

– to assess the applicability of the obtained results for clinical use.

4. Materials and methods of research

Recorded changes in potentials from the surface of the human chest obtained at different frequencies f_i of injected current I in accordance with the program of experimental studies are used as the source data for theoretical studies. The organization of the process of collecting measurement data, their processing and visualization were performed using a multi-zone information and measurement system of multi-frequency electric impedance tomography (IMS of MF EIT).

To simulate ventilation measures, we used a load testing procedure, which was performed using the Coach 2 medical incentive spirometer. This device is widely applied in the clinical practice of intensive spirometry to restore lung function of patients in the postoperative period (in the clinic or at home).

Computational experiments were performed using the Statistica applied software package (USA), MS Excel environment (USA), MATLAB (USA).

Experimental studies were conducted on volunteers from the developers of the IMS of MF EIT. All of them gave individual information written consent to participate in the tests on the basis of the laboratory of information and measuring systems for medical purposes of the SRSPU (SPI) (Novocherkassk). The basic source data for experimental studies are shown in Table 1.

Table 1

Basic source data for experimental studies

No. by order	Name	Description
1	2	3
1	Number of test participants	3 people, volunteers (who gave written consent to participate in experimental studies). For convenience, each test participant was assigned the following designations – $P1$, $P2$, and $P3$
2	Distinctive features of test participants	Young people under 35, having different physiques. Males. Without pathologies of respiratory function and breathing function. The SpO2 level before and after doing research in all subjects is not less than 99 %
3	Range of inhaled air, V	from 500 ml to 4,000 ml. It is determined by the functionality of the used device to perform breathing maneuvers. Pitch of increase ΔV=500 ml
4	Device for breathing maneuvers	Incentive spirometer Coach 2
5	Contraindications to the use of the device	There are no contra indicators to apply this incentive spirometer
6	Specificity of respiratory movements when performing breathing maneuvers	Active inhalation, passive exhalation

Continuation of Table 1

1	2	3
7	Tested EIT device	Information-measuring system of multi-frequency electric impedance tomography (IMS of MF EIT). Includes a current source proposed in [10], but modified for use in the IMS of MN EIT
7. 1	Amplitude of injected current, I	5 mA (at each frequency from the specified frequency range)
7. 2	Frequency of injected current, f_i	from 50 kHz to 400 kHz, with the pitch Δf=50 kHz
7. 3	System of connections of the EIT (Circuit of injection and measurement)	To perform research at all frequencies, the circuit of «adjacent electrodes» was used
7. 4	The type of the used electrode belt of the EIT	The electrode belt consisting of single-use electrodes was manufactured. The number of electrodes in the belt is 16 pcs
8	Place of theoretical and experimental research	Laboratory of «Information and Measurement Systems for Medical Purposes». Novocherkassk, Rostov region, SRSPU (SPI)
9	Principal researcher	Grayr Karenovich Alexanian
10	The position of the test participant in space when performing a breathing maneuver and EIT examination	Only in the standing position. Holding a load spirometer in the hand
11	Terms of experiments	December 2020
12	Duration of any cycle of experiments	1 (one) day per one test participant, no more than 8 hours for the entire complex of EIT examination in order to observe the minimum spread of time of physiological parameters of vital activities of an organism
13	Number of repeated tests at each frequency and in established respiratory volume	5 (five) tests followed by their simple averaging at each frequency and in the established respiratory volume

All manipulations and activities related to the research involving healthy volunteers were performed only after obtaining their written consent. The criteria for inclusion of volunteers in the studies were the following: healthy adult young people chosen from the developers of the IMS MF EIT, who themselves gave written informed consent to participate in the tests. The criteria for exclusion from participation in experimental studies were the existence of an implanted pulse generator, surgeries in the chest area, existence of skin injuries, health deterioration. The process of performing experimental studies was accompanied by continuous recording of the obtained data, taking into consideration all the specific features of the experiment. Simultaneously with the automatic registration of changes in the potentials of the MF EIT for each subject ($P1$–$P3$), the results of the EIT examination at a given frequency of injected current were recorded manually.

Measurement data of the MF EIT were processed, conductivity field was reconstructed, dynamic visualization of the results of calculation of ventilation, perfusion, and the ventilation-perfusion ratio was performed based on the software for controlling the operation of the IMS of MF EIT and the user interface developed by the authors. Secondary additional statistical processing was performed using a specialized software package STATISTICA.

quency electric impedance tomography. This makes it possible to simulate the AVL process involving a healthy person and to link the assigned respiratory volume to measurement data. In this case, the active element that controls inhalation and exhalation processes is the test participant himself, who uses an incentive spirometer for research purposes. The general circuit explaining the basic principles of obtaining and processing measurement data is shown in Fig. 1.
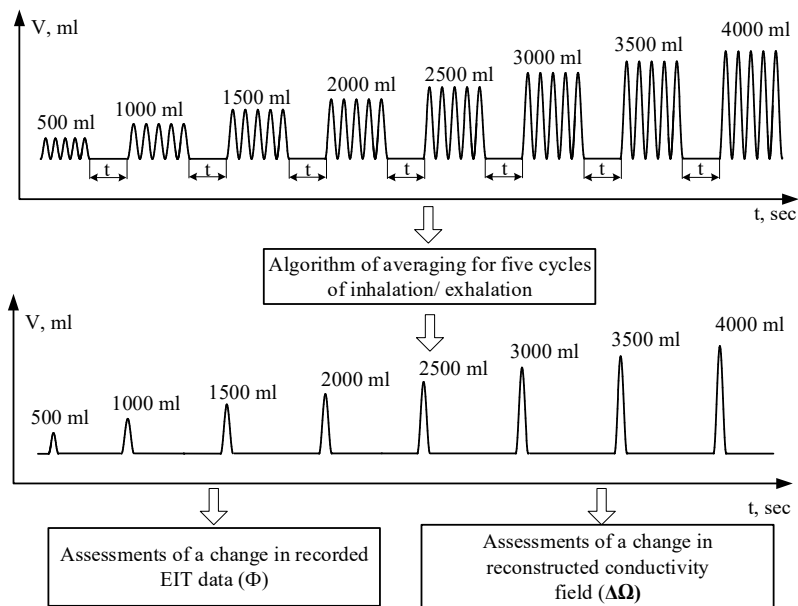

Fig. 1. General circuit explaining the basic principles of obtaining and processing measurement data in the framework of experimental studies

5. Experimental evaluation of dependence of measurement data on the volume of inhaled air

5. 1. General plan of experimental studies

The essence of experimental studies is controlled filling of lungs with fixed air volume V_i while performing multi-fre-

It schematically shows the breathing pattern used in the study. During the experiment, each test participant (code designation $P1$, $P2$, and $P3$ is accepted) must perform a controlled series of five inhalations/exhalations on each of the volumes set on the incentive spirometer V_i (from 500 ml to 4,000 ml, with a pitch of increase

of 500 ml). To decrease the methodological error and filtration of interference associated with the subjective features of using Coach 2, caused by the failure to reach or by exceeding the set volume of V_i. the measurement data for each volume of V_i were averaged. The standing position was chosen for the convenience of the test participant performing a breathing maneuver and the MF EIT. In subsequent studies, only averaged data were used as the source data to reconstruct the conductivity field and to assess a change, as well as to estimate changes in measurement information.

Each test participant performed breathing maneuvers using the Coach 2 simulator for three weeks (with a frequency of repetition of 1 time in 3 days) performed breathing maneuvers using the Coach 2 simulator. This was done in order to eliminate discomfort, improve the convenience and predictability of the experiment, as well as study the problematic moments that may occur during tests. For each test participant $P1$, $P2$, and $P3$, new incentive spirometers Coach 2 and the means for their cleaning and disinfection were purchased. During the tests, it was found that between controlled breathing maneuvers, it is desirable to choose an interval of at least $t=1$ minute. A general block diagram of the implementation of experimental studies, adjusted according to the results of tests, is shown in Fig. 2.

Each frequency of injection current was set by the principal researcher on the sensor monitor IMS of MF EIT. The principal researcher also monitored the progress of the experiment, recorded the results, and monitored compliance with the sequence of actions according to the plan formed in advance. The pitch of increasing the injection frequency Δf was 50 kHz. The pitch of setting the respiratory volume ΔV was 500 ml. Upon completion of the experimental studies, as well as after each test participant, the IMS of the MN EIT was turned off, the electrode system was disassembled and sent for disinfection, the used electrodes were disposed of.

5. 2. Determining the dependence of measurement data on the volume of inhaled air and frequency of the injected current

5. 2. 1. Instrument base and source data for research

Table 2 shows the list of the equipment and the components that are directly used to obtain measurement data of the MF EIT.
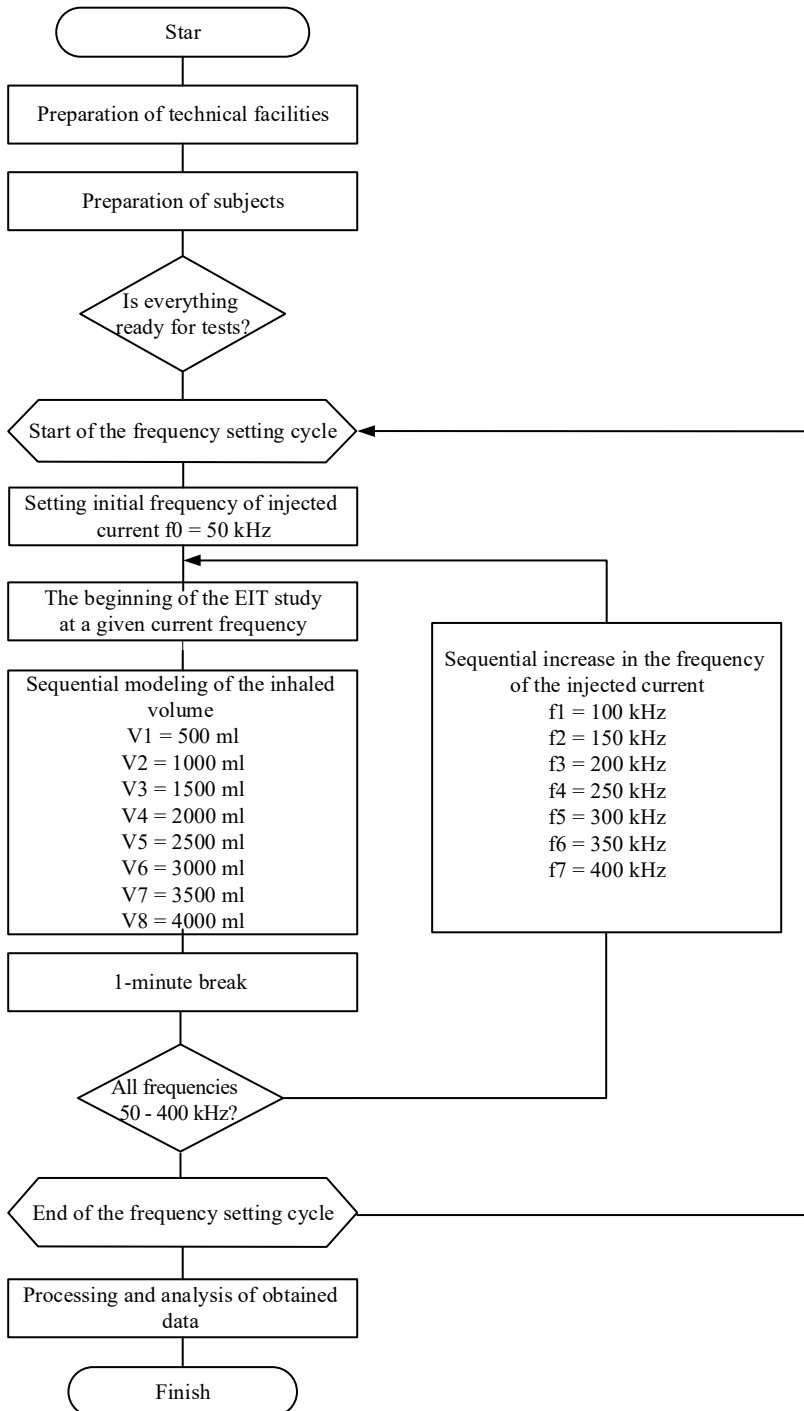
Table 2

Basic source data for experimental studies

Type of equipment/parts	Type of equipment/parts
Incentive spirometer	Coach 2
Information and measurement system of multifrequency electric impedance tomography of human lungs	IMS MF EIT
Disposable ECG electrodes	produced by *Scintac* (re-sticking to the surface of the body is not allowed)

Fig. 3 shows the view of the experimental setup and its main parts.

New spirometers were purchased for each test participant. Disposable electrodes were used as part of the electrode system (Fig. 3, *c*).
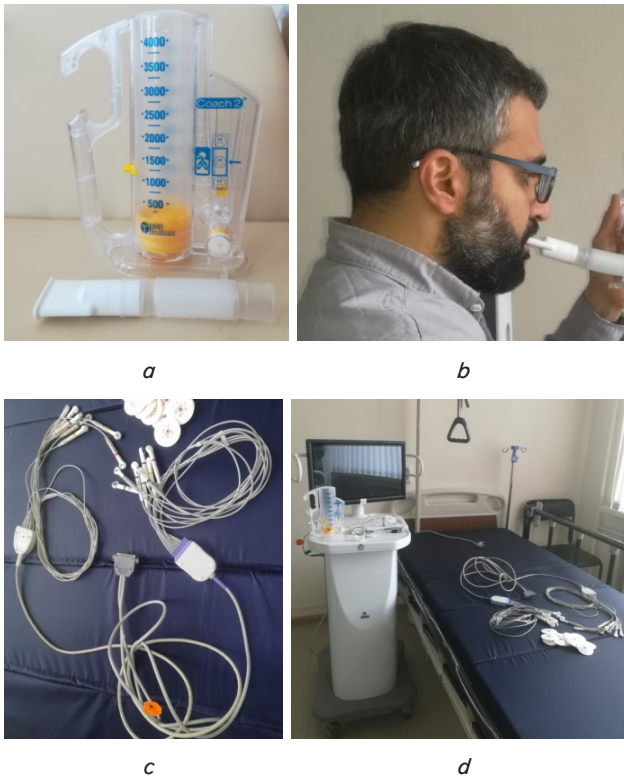

Fig. 2. Block-diagram of the generalized algorithm for obtaining measurement data

Fig. 3. General view of the experimental setup and its parts:
a — view of the incentive spirometer Coach 2; *b* — example
of using incentive spirometer Coach 2 in the framework of
these studies (the photo shows the author); *c* — view of the
electrode system with disposable electrodes; *d* — view of the
developed information and measurement system of electric
impedance tomography

5. 2. 2. Features of participation of volunteers in experimental studies

We wrote a brochure of the experiment, with which each of the participants got acquainted. We received written consent from each participant $P1$, $P2$, and $P3$ to take part in the experiment. The incentive spirometer Coach 2, which is a non-sterile product for individual use of respiratory therapy and has an inhalation port, was chosen to perform controlled breathing maneuvers. Incentive spirometers Coach 2 are designed to be used in intensive spirometry. The product helps to restore patients after operations and/or if necessary, to do deep breathing exercises with the possibility of subjective control of inhaled volume. In accordance with the instruction manual, incentive spirometers Coach 2 are designed to be used in medical institutions or at home.

During the measurements, $P1$, $P2$, and $P3$ did not eat, drink water, perform any physical exercises and other actions that could distort the results. The obtained data were automatically saved with the possibility of reproduction and processing in outside specialized packages of applied programs.

5. 2. 3. General principles of obtaining measurement information

Measurement information is obtained based on the EIT algorithms, which include injecting current through an object and recording the response to this influence. Their practical implementation is aimed at performing the following main stages:

– superimposition of electrodes distanced from each other and closely connected to each other along the perimeter of an object;

– connection of the current source to a pair of adjacent electrodes and injection of high-frequency current of small amplitude I through an object;

– recording the changes of potentials on all other electrodes that are not injectable at the given moment;

– connection of the current source to the next pair of adjacent electrodes and recording the changes of potentials Φ on all electrodes that are not currently injected.

The stages of switching electrodes, injection, and collection of measurement data Φ are continuous and are repeated until the device stops working. As a result, an array of measurement information, which is the changes of the potentials Φ from the surface of an object obtained during the observation period, is collected. Their magnitude depends on the functioning of an object and its structure. Further, based on this information, the inverse problem is solved in order to reconstruct changes in the internal conductivity field of object Ω. The EIT method is most widely used in medicine for monitoring the lung function of a person connected to an AVL apparatus or having respiratory support. This is caused by the fact that the intake of air in the lungs is a periodic process in which an object with low resistance (lung tissue) receives a volume of the respiratory mixture or air V_i with resistance that is many times greater than its own. As a result of monitoring the changes in conductivity field Ω in the plane of putting of the electronic system, it is possible to visualize those parts of the lungs that, for example, are not involved in ventilation. At the same time, pain is excluded, a test participant does not feel the passage of current, and the monitoring itself can be performed for a long time, at the bedside and in conjunction with other medical products connected to a patient (except for the defibrillator of an electrosurgical knife).

In the general case, the fixed-frequency current is injected through a patient. In the case of the MF EIT, it is proposed to use a frequency range with a fixed pitch of increase. Due to this, it is possible to read measurement data, which contain, among other things, information about the dependence of the electrical properties of a research object on frequency. Thus, one can get an additional channel of useful diagnostic information, which is peculiar to a particular person, and personalize the EIT examination.

5. 3. Processing and analysis of the obtained measurement information

The process of obtaining an array of measurement data Φ for given volume V_i is a continuous cycle of obtaining changes in the difference of potentials from the electrodes in accordance with the selected system of EIT connections (1).

$$\Phi_{f_i}^{V_i} = \sum \left| \phi_{j+1} - \phi_j \right|, \tag{1}$$

where $\left(\phi_{j+1} - \phi_j \right)$ is the recorded measurements of the difference of potentials of the EIT, $j=1...N$, where N is the total number of electrodes, $N=16$; V_i=[500 ml; 1000 ml; 1500 ml; 2000 ml; 2500 ml; 3000 ml; 3500 ml; 4000 ml]; f_i=[50 kHz; 100 kHz; 150 kHz; 200 kHz; 250 kHz; 300 kHz; 350 kHz; 400 kHz].

The results of experimental data at different values of respiratory volumes and at different frequencies of injected

current were obtained for each of the test participants $P1$, $P2$, and $P3$. The data were obtained. Subsequently, according to the circuit presented in Fig. 1, the array of measurement data $\Phi_{f_i}^{V_i}$ was averaged according to formula (2).

$$\Phi_{cp} = \frac{\sum \Phi_{f_i}^{V_i}}{K},\tag{2}$$

where K is the number of all $\Phi_{f_i}^{V_i}$, obtained at assigned V_i and f_i.

Fig. 4–6 show the dependence of Φ_{cp} (ordinate axis) on the magnitude of respiratory volume V_i (abscissa axis) at different frequencies of injection current f_i for each test participant $P1$, $P2$, and $P3$.

Analyzing the content of Fig. 4–6, a, it can be concluded that there is an increase in the value of Φ_{cp} depending on the magnitude of respiratory volume V_i. At the same time, within the fixed V_i, a decrease in the magnitude of Φ_{cp} is clearly noticeable, in this case, each of $P1$, $P2$, and $P3$ has his own rate of its change. If we consider the change of conductivity field Ω of the test participants performing breathing maneuvers, it is possible to observe a decrease in its magnitude at an increase in V_i. Within a fixed V_i. there is a clearly noticeable increase in Ω at an increase in the frequency of injection current f_i.

Fig. 7 shows the dependence of the measured values of changes in the EIT potentials on the frequency of injected

current f_i for different respiratory volumes V_i in three test participants.

The results of processing the measuring data shown in Fig. 7, make it possible to conclude that the results obtained fully comply with theoretical studies on changing the electrical properties of living biological tissues when an alternating electric current passes through them. It is noticeable that each test participant, under fixed conditions of the experiment, is different as for the levels of measurement data. This is due to the internal structure and composition of the tissues of the body (thickness of adipose tissue, geometric dimensions of lungs, the perimeter of the chest girth, etc.) of each out of $P1$, $P2$, and $P3$.

Fig. 7 demonstrates that possible artifacts in the course of obtaining measurement data can lead to misinterpretation of the data (the lower group of diagrams for $P3$ has a surge at a frequency of 150 kHz). In this regard, it is necessary to introduce a unit for tracking and analyzing the correctness of data at the MF EIT (for example, along with control of the quality of electrode fastening) into the algorithms for performing MF EIT

Based on the obtained measurement data $\Phi_{f_i}^{V_i}$ at different frequencies of injected current and inhaled volumes, the conductivity field was reconstructed using the EIT method. In general, this stage of processing measurement data can be represented in the form of (3):

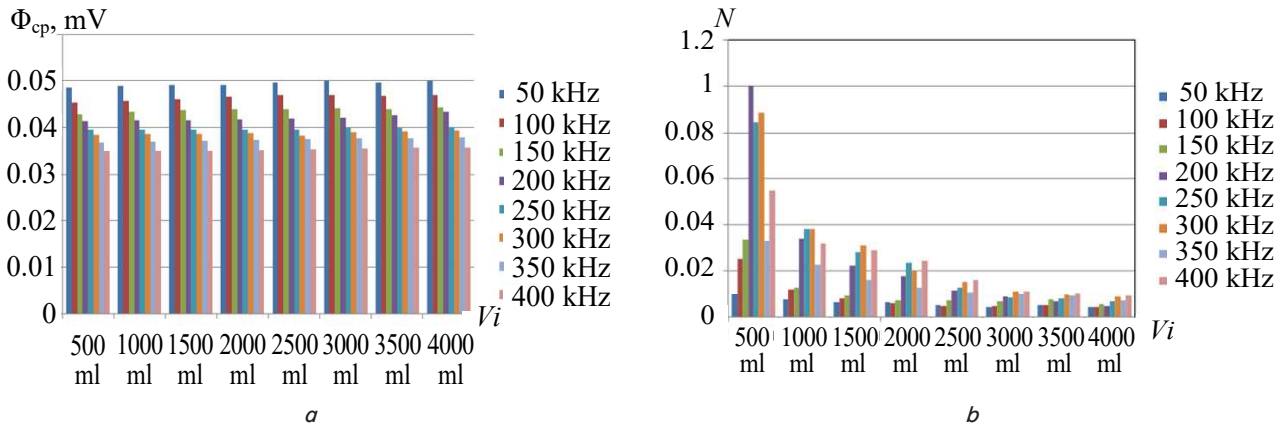$$\Phi = \Phi_{f_i}^{V_i} \rightarrow \Omega_{f_i}^{V_i} = \Omega.\tag{3}$$

Fig. 4. For test participant $P1$: a — dependence of Φ_{cp} on the magnitude of respiratory volume V_i at different frequencies f_i; b — the normalized values of a change in conductivity Ω of the region of placing the electrode system (N) at different frequencies of injection current f_i at assigned V_i
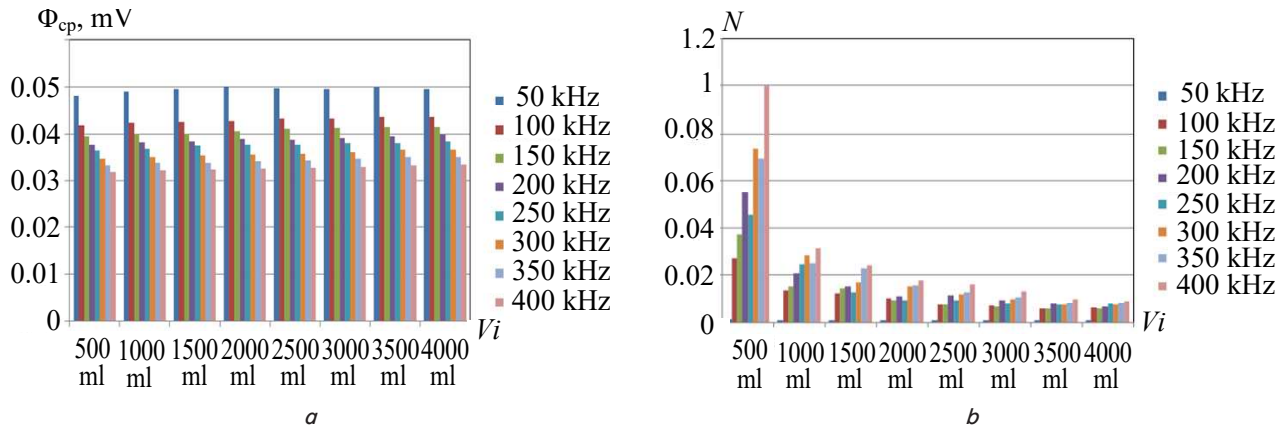

Fig. 5. For test participant $P2$: a — dependence of Φ_{cp} on the magnitude of respiratory volume V_i at different frequencies f_i; b — the normalized values of a change in conductivity Ω of the region of placing the electrode system (N) at different frequencies of injection current f_i at assigned V_i
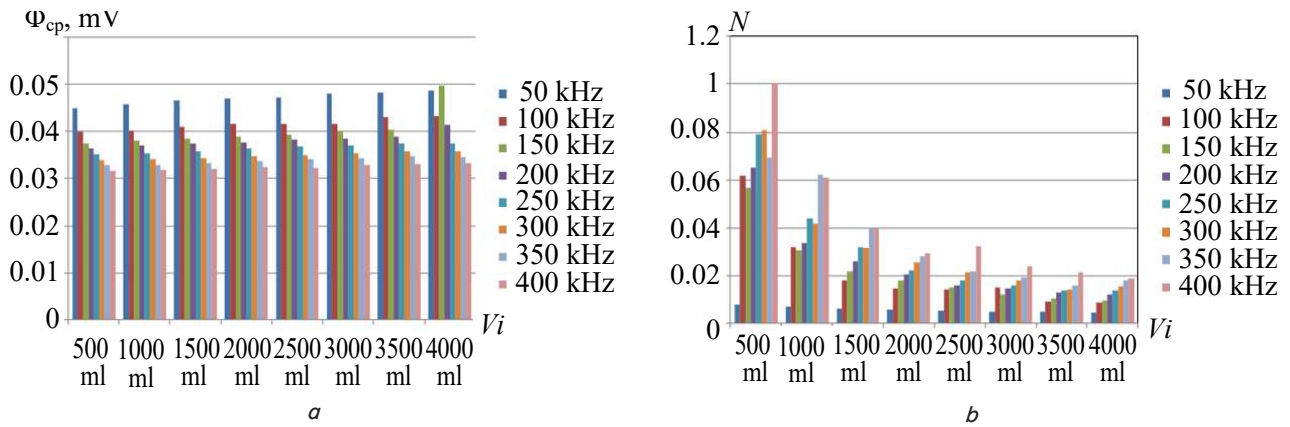
Fig. 6. For test participant $P3$: a — dependence of Φ_{cp} on the magnitude of respiratory volume V_i at different frequencies f_i; b — the normalized values of a change in conductivity Ω of the region of placing the electrode system (N) at different frequencies of injection current f_i at assigned V_i
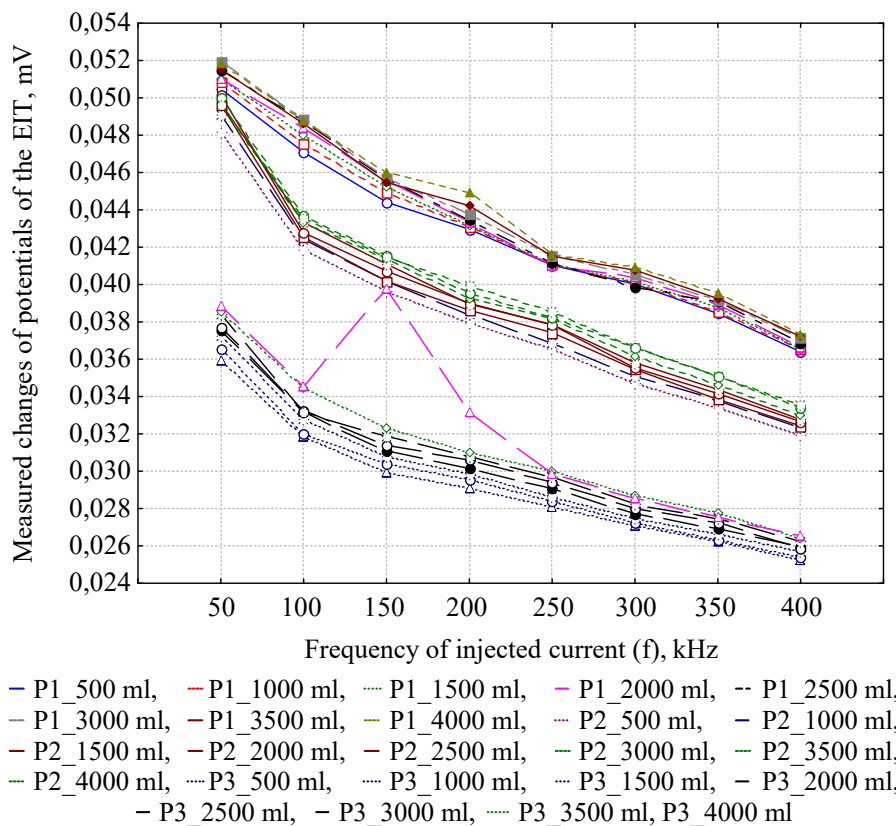

Fig. 7. Dependence of the measured values of changes of potentials in electrical impedance tomography on the frequency of injected current f_i for different respiratory volumes V_i in three test participants ($P1$, $P2$, and $P3$)

As a result, we obtained an array $\Omega_{f_i}^{V_i}$, reflecting the relative change in conductivity field (in the cross-section of placing the electrode system) for different frequencies of injected current and inhaled volumes. Here and further, for the convenience of designating the axes of the diagram, a simplified designation was adopted – Ω and Φ.

Fig. 8, a shows the diagrams of the spread of the dependence of recorded changes in EIT potentials on the volume of inhaled air Vi. Fig. 8, b shows the dependence of the calculated values of a change of the reconstructed conductivity field Ω of the test participants. The data in Fig. 8 are presented for all test participants $P1$, $P2$, and $P3$.

Analyzing the data in Fig. 8, it can be concluded that a characteristic feature for all test participants is a large spread at the

lower frequencies, especially at injection frequency f_0=50 kHz. This will lead to the conclusion that for $P1$, $P2$, and $P3$ the MF EIT should not be performed at low injection frequencies, especially at frequency f_0. In this regard, it is necessary to correct the algorithm for performing MF EIT with adjustment for possible injection frequencies, at which the greatest spread is observed. This recommendation requires more detailed scientific theoretical and applied research, including physiological studies. In addition, the spread (sweep) diagrams reflect differences between $P1$, $P2$, and $P3$ as for electrical properties. At the same time, the nature of the change in the measurement data of the EIT at an increase in the volume of inhaled air is the same for all subjects. Thus, the implementation of the multi-frequency principle makes it possible to differentiate between the

subjects in order to increase the degree of personalization of the EIT examination.

Further, to enhance the visibility of the results of experimental tests, cluster analysis was applied to the obtained array of measurement data Φ for each $P1$, $P2$, and $P3$. Cluster analysis makes it possible to objectively systematize the obtained results of the study and give a simplified idea of the nature of a change in measurement data and a change in reconstructed conductivity field at an increase in the frequency of injected current f_i.

Fig. 9 shows the results of cluster analysis of measurement data at different frequencies of injected current. Fig. 10 shows the results of cluster analysis of changes in the reconstructed conductivity field at different frequencies of injected current.

The results of processing and analysis of Φ and Ω make it possible to conclude that at MF EIT, the measurement data obtained directly from the MF EIT device and not subjected to post-processing reflect the characteristics of the object of research. They can serve as an additional channel for obtaining basic information to account for artifacts, as well as to increase the correctness of reconstruction tasks.

Analyzing the content of Fig. 7–10, it can be concluded that the MF EIT is an effective tool for objective reliable differentiation of patients. Its application in the tasks of EIT of human lungs makes it possible to increase the degree of personalization of the procedure and minimize artifacts in the source data of the EIT.
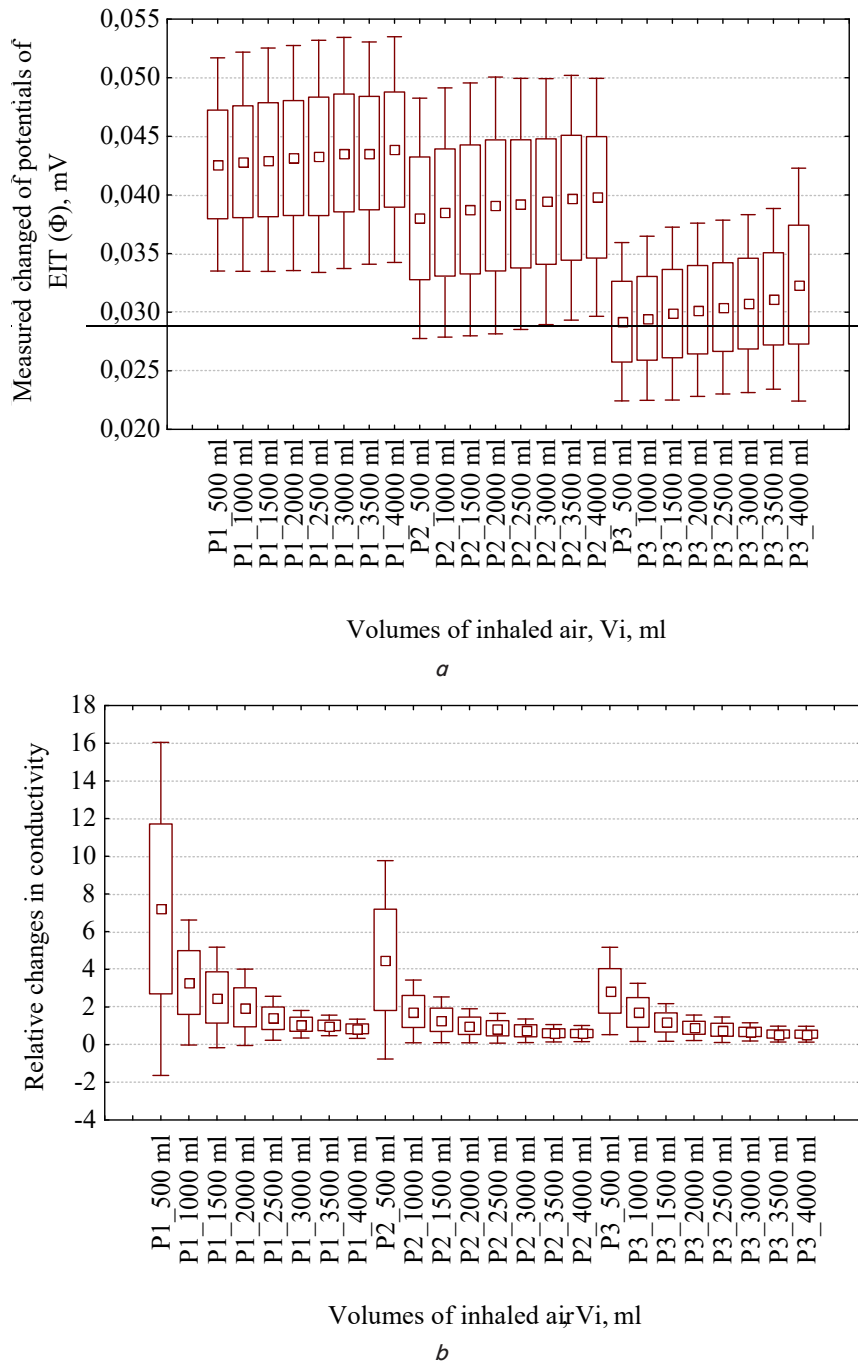

Fig. 8. Spread diagrams for test participants $P1$, $P2$, and $P3$: a — dependence of recorded changes in EIT potentials (Φ) on the volume of inhaled air; b — dependence of calculated values of changes in reconstructed conductivity field (Ω) on the volume of inhaled air Vi
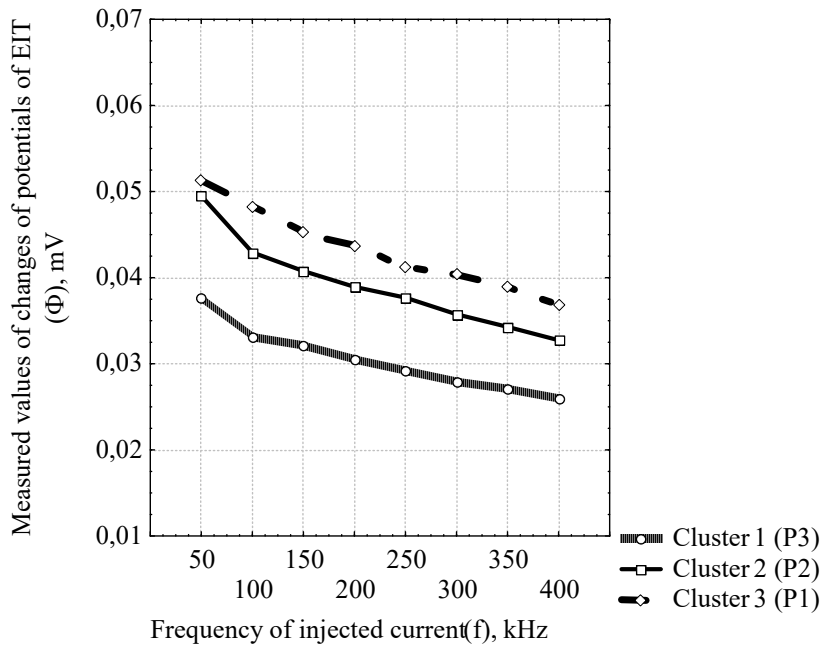
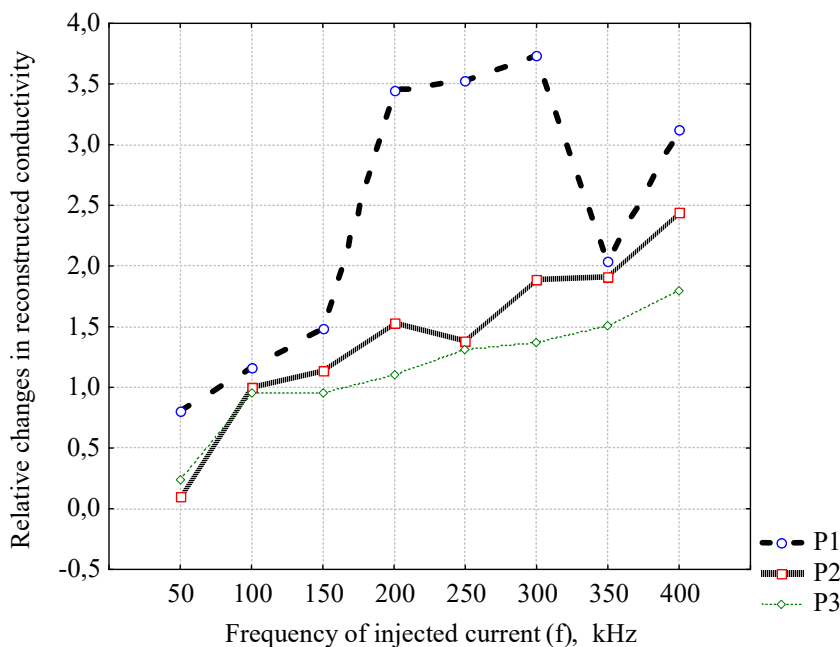Fig. 9. Results of cluster analysis of measurement data Φ at different frequencies of injected current f_i

Fig. 10. Results of cluster analysis of reconstructed conductivity field Ω at different frequencies of injected current f_i

state of a patient and the parameters of the impedance of the field of research peculiar to him. This can be caused for various reasons, for example, under the influence of drug therapy, drop infusion, or various kinds of manipulation with the patient's position in space, etc. Multifrequency electric impedance tomography can serve as one of the ways to solve the above problems.

The practical implementation of the MF EIT of the human lungs does not create additional inconvenience to a patient and medical personnel. All the test participants pointed out the absence of discomfort and inconvenience. In addition, the process of air filling of lungs was intuitively and clearly visualized in a dynamic image in accordance with the volume of incoming air at all frequencies and at all specified volumes.

6. Discussion of results of experimental studies of the dependence of measurement data on the volume of inhaled air

The proposed approach to performing the MF EIT with the simultaneous task of controlled respiratory volume showed positive results of the practical use of an incentive spirometer for simple modeling on a healthy person of the AVL mode. This significantly expands the range and directions of further non-invasive studies of the EIT method to solve the problems of long-term bedside monitoring (both pre-and postoperative). Nevertheless, the obtained results enable us to conclude that healthy subjects in the conscious state may well act as a measure of objective control, and their subjective assessments can be systematized for subsequent comprehensive analysis.

The obtained results of experimental studies (Fig. 4–6) show that there is a dependence of the magnitude of measurement data both on the volume of inhaled air and on the frequency of the injected current. This feature can be used to develop a number of medical devices for personalized monitoring of human lung function. This is achieved due to the identified sensitivity of the MF EIT itself to the internal structure of the research object and to the modes of its functioning.

5. 4. Assessment of applicability of obtained results for clinical use

The obtained results can serve as the basis for the development of a method for personalization of the EIT activities, including those in solving problems of pre-and postoperative monitoring of human lung function. The essence of the method is as follows. Initially, before performing surgical interventions, an adequate injection rate for a particular patient is evaluated. Then, in the postoperative period, it is considered as a reference for the launch of the EIT examination. This makes it possible to overcome the problem associated with the fact that when performing resuscitation measures, there is inevitably a distortion of objective information about the

The results of the studies, systematized in Fig. 7, 8, reflect the full compliance of analytical expressions – an increase in the difference in recorded potentials is associated with an increase in the volume of supplied air. At the same time, at an increase in the frequency of the injected current, we observe a decrease in the magnitude of measurement data.

Analyzing the diagrams of dependences shown in Fig. 7, 10, it can be concluded that it is necessary to introduce a unit for tracking and analyzing the data correctness

at the MF EIT (for example, along with control of the quality of electrode fastening) into the algorithms of performing the MF EIT. This will make it possible to select problem areas in the array of measurement data before launching processing and to take them into consideration when analyzing the reconstructed field.

It was revealed that there are frequencies at which the maximum spread of measurement data is observed according to the results of a series of repeated experiments (Fig. 8). At the same time, the nature of a change in measurement data of the EIT at an increase in the volume of inhaled air is the same for all test participants. It is assumed that this feature can also be used to increase the degree of EIT personalization. For example, identification of the frequency range with the maximum spread may indicate the inadequacy of the specified parameters of the EIT examination for a particular test participant. Or vice versa, the search for the frequency (or frequency range), after which there is a minimum standard deviation of the measurement data of the MF EIT.

It should be noted that the previously developed IMS of MF EIT showed high operation stability, regardless of the physiological characteristics of a test participant. It was experimentally established that it can be applied to perform an EIT examination on ventilation volumes from 500 ml to 4,000 ml. Obtaining the dependence of changes of potentials at different frequencies and at different respiratory modes make it possible to conclude that the proposed IMS of MF EIT can be used in further work on the study of the modes and features of the MF EIT.

It should be noted that these studies have a series of limitations. These include a small sample size of test participants, which requires a performance check on a larger group, as well as the absence of test participants with problems with external respiratory function. However, these works are planned to be performed on the basis of a medical organization with the involvement of real patients of an intensive care unit. In addition, within the framework of these studies, the tasks were set for the study of the MF EIT on healthy subjects who do not have problems with lung function. This was done in order to assess the sensitivity of the EIT method.

The issue of using the MF of EIT for the tasks of assessing lung perfusion by the MF EIT method, as one of the directions of application of the multi-frequency mode, remains unclear. It is important to conduct experimental and clinical studies and to explore the problem of the use of the MN EIT in intensive care units. In particular, it is necessary to assess the impact of third-party medical devices on the results of the MF EIT.

The disadvantages of this study include the following features: a limited frequency range (from 50 kHz to 400 kHz), a frequency increase pitch that is multiple of 50 kHz, fixed current force of 5 mA. These problems and limitations are the subjects of further research, require separate algorithmic solutions, and go beyond the scope of this paper.

Among the main difficulties in the development of this direction, it is possible to single out a weak methodological study of the subject area due to the relatively short terms of research in the direction of the MF EIT under clinical conditions.

forming the MN EIT, was proposed. This makes it possible to simulate the AVL process on a healthy person and link the specified respiratory volume to measurement data. In this case, the active element that controls the processes of inhalation and exhalation is a test participant himself, who uses an incentive spirometer for research purposes. Thus, the proposed method enables conducting preclinical studies of systems and methods of the MF EIT on healthy people and to obtain measurement information with maximum adequacy to the object of study.

2. Experimental studies were carried out to determine the dependence of measurement data on the volume of inhaled air and the frequency of the injected current. The tests were conducted involving three volunteers from the developers of the IMS of MF EIT, who gave written informed consent to participate in the experiment. Experimental studies were conducted at the frequency of the injected current from 50 kHz to 400 kHz (with an increase pitch of 50 kHz) and at respiratory volumes from 500 ml to 400 ml (with an increase pitch of 500 ml). As a result, measurement information was collected and systematized in the form of changes in EIT potentials for these frequencies and volumes. Thus, experimental data on the simultaneous performance of the MF EIT at different respiratory volumes were collected. Various algorithms of processing and analysis can be applied to them in order to identify existing dependences and features.

3. The obtained measurement information for each test participant at different values of respiratory volumes and at different frequencies of injected current was processed and analyzed. It was established that there is an increase in the value of measurement data depending on the magnitude of respiratory volume. At the same time, within a fixed volume, a decrease in the magnitude of changes of the EIT potentials is clearly noticeable, and the rate of its change is different for all test participants. When assessing the change in the reconstructed conductivity field, it was found that there is a decrease in its magnitude at an increase in respiratory volume. At the same time, within a fixed respiratory volume, an increase in conductivity field is clearly noticeable with an increase in the frequency of the injected current.

It was revealed that for all test participants, the maximum spread of changes in EIT potentials is observed at low frequencies, especially at the injection frequency of 50 kHz. This means that for these people, EIT should not be performed at low injection rates. A recommendation on the need to adjust the algorithm for performing the MF EIT taking into consideration possible injection frequencies, at which the greatest variation is observed, was made.

4. The main directions of applicability of the obtained results for clinical use were considered. It was shown that at the MF EIT, measurement data obtained directly from the MF EIT device and not subjected to post-processing reflect the features of the object of study. They can serve as an additional channel for obtaining basic information for accounting for artifacts, as well as for increasing the correctness of algorithms for solving inverse problems that are used to reconstruct the conductivity field.

7. Conclusions

1. A general plan of experimental studies, involving the controlled filling of lungs with a fixed air volume while per-

Acknowledgments

References

1. Pekker, Ya. S., Brazovskiy, K. S., Usov, V. N. (2004). Electrical impedance tomography. Tomsk: NTL, 192.
2. Bachmann, M. C., Morais, C., Bugedo, G., Bruhn, A., Morales, A., Borges, J. B. et. al. (2018). Electrical impedance tomography in acute respiratory distress syndrome. Critical Care, 22 (1). doi: https://doi.org/10.1186/s13054-018-2195-6
3. Brabant, O., Crivellari, B., Hosgood, G., Raisis, A., Waldmann, A. D., Auer, U. et. al. (2021). Effects of PEEP on the relationship between tidal volume and total impedance change measured via electrical impedance tomography (EIT). Journal of Clinical Monitoring and Computing. doi: https://doi.org/10.1007/s10877-021-00651-x
4. Lobo, B., Hermosa, C., Abella, A., Gordo, F. (2018). Electrical impedance tomography. Annals of Translational Medicine, 6 (2), 26. doi: https://doi.org/10.21037/atm.2017.12.06
5. Frerichs, I., Amato, M. B. P., van Kaam, A. H., Tingay, D. G., Zhao, Z. et. al. (2016). Chest electrical impedance tomography examination, data analysis, terminology, clinical use and recommendations: consensus statement of the TRanslational EIT developmeNt stuDy group. Thorax, 72 (1), 83–93. doi: https://doi.org/10.1136/thoraxjnl-2016-208357
6. Crivellari, B., Raisis, A., Hosgood, G., Waldmann, A. D., Murphy, D., Mosing, M. (2021). Use of Electrical Impedance Tomography (EIT) to Estimate Tidal Volume in Anaesthetized Horses Undergoing Elective Surgery. Animals, 11 (5), 1350. doi: https://doi.org/10.3390/ani11051350
7. Lee, M. H., Jang, G. Y., Kim, Y. E., Yoo, P. J., Wi, H., Oh, T. I., Woo, E. J. (2018). Portable multi-parameter electrical impedance tomography for sleep apnea and hypoventilation monitoring: feasibility study. Physiological Measurement, 39 (12), 124004. doi: https://doi.org/10.1088/1361-6579/aaf271
8. Tomicic, V., Cornejo, R. (2019). Lung monitoring with electrical impedance tomography: technical considerations and clinical applications. Journal of Thoracic Disease, 11 (7), 3122–3135. doi: https://doi.org/10.21037/jtd.2019.06.27
9. Longhini, F., Maugeri, J., Andreoni, C., Ronco, C., Bruni, A., Garofalo, E. et. al. (2019). Electrical impedance tomography during spontaneous breathing trials and after extubation in critically ill patients at high risk for extubation failure: a multicenter observational study. Annals of Intensive Care, 9 (1). doi: https://doi.org/10.1186/s13613-019-0565-0
10. Aleksanyan, G. K., Shcherbakov, I. D., Kucher, A. I. (2017). Feature research of using current source in 2-dimensional and 3-dimensional multifrequency electrical impedance tomography devices. Journal of Engineering and Applied Sciences, 12 (3), 587–592. Available at: http://docsdrive.com/pdfs/medwelljournals/jeasci/2017/587-592.pdf